Adaptive Finite Element Methods for Conservation Laws

Claes Johnson

Mathematics Department
Chalmers University of Technology
412 96 Göteborg, Sweden

Abstract. The purpose of this chapter is to give an introductory overview of our recent work together with coworkers on computational methods for conservation laws, which are reliable in the sense that the computational error may be controled on a given tolerance level in a given norm, and efficient in the sense that the desired error control may be achieved at (nearly) minimal computational cost. To satisfy the desired criteria of reliability and efficiency, the computational methods are adaptive with feed back from the computational process. The adaptive methods are based on a posteriori error estimates, where the error is estimated in terms of the mesh size, the residual of the computed solution, and certain stability factors measuring relevant stability properties of the solution being approximated through the solution of an associated linearized dual problem. The a posteriori error estimates give stopping criteria guaranteeing the desired error control, and also serve as part of the modification criteria for adaptively choosing the computational mesh. We prove analytically that the stability factors in the basic model cases of shocks and rarefactions in one dimension, are of moderate size. We also present results from numerical computations of dual solutions and stability factors.

1 Introduction

In this chapter we give an introductory overview of our recent work together with E. Burman, P. Hansbo, M. Larson, R. Sandboge, and A. Szepessy, on computational methods for conservation laws, which are *reliable* in the sense that the computational error may be controled on a given tolerance level in a given norm, and *efficient* in the sense that the desired error control may be achieved at (nearly) minimal computational cost. To satisfy the desired criteria of reliability and efficiency, the computational methods are *adaptive* with *feed back* from the computational process. Key references to this work includes [23], [19]-[21], [32], [33], [37], [2], [3], [34]. The presented work is part of a larger program on adaptive computational methods for differential equations based on generalized Galerkin methods outlined in [8], presented in [9]-[18], [27], [28], [30], [31], [35], and further developed in the series of books [4]-[7], and realized in the related software *Femlab* (http://www.md.chalmers.se/Math/Research/Femlab/), and *Mechlab* ([29]. We refer the reader to these sources for a more complete account of our work.

Conservation laws are systems of nonlinear partial differential equations on *conservation form*:

$$\frac{\partial u}{\partial t} + \sum_{j=1}^{3} \frac{\partial}{\partial x_j} f_j(u, x, t) = S(u), \tag{1}$$

where $u = u(x, t)$ is a vector function depending on the Euclidean space coordinate $x \in \mathbb{R}^3$ and time variable $t > 0$, the f_j are given flux vectors depending on (u, x, t) and include both convective and diffusive effects, and $S(u, x, t)$ is a given source vector. The *Navier-Stokes equations* for incompressible and compressible fluid flow take this form with u representing mass, momentum and energy, and (1) expressing conservation or balance laws for u, and the source term $S(u)$ representing exterior forces. In generalizations including chemical reactions and multi-phase flow, u includes the different mass fractions and $S(u)$ includes reaction or interaction terms. The inviscid form of the Navier-Stokes equations with diffusive viscosities equal to zero, is referred to as the *Euler equations*.

We consider the problem of reliable and efficient numerical computation of solutions of conservation laws, including the Euler and Navier-Stokes equations, which we may refer to as the problem of *computability* of solutions of conservation laws. We say that a certain solution u is *computable* with a given amount of computational work if

$$\|u - U\| \leq TOL, \tag{2}$$

where $\|\cdot\|$ is a given norm, TOL is a a given tolerance, and U is an approximation of u computed with the given work. This problem is intimately connected to the mathematical problem of existence, uniqueness and stability of the solution u. Clearly, a solution must exist to be computable, and because of the approximate nature of computed solutions, the concept of *stability* measuring the distance between solutions with nearby data, is central. There are results indicating that the viscid Navier-Stokes equations have unique solutions even for large time and data, but quantitative a priori information on stability is very sparse. It appears that as the viscosity decreases, in general the complexity of solutions increases and their stability deteriorates, corresponding to the development of fluctuating turbulent solutions with very fine-scale features. Accordingly, the work to compute solutions within a given tolerance, in general increases with decreasing viscosity. For the Euler equation limit with zero viscosity, existence and uniqueness may be seriously questioned, as well as of course the computability of solutions. It may be argued that real physical processes always involve some viscous effects, and thus it appears that the natural object of study is the Navier-Stokes equations.

Paradoxically, the development of computational methods for conservation laws initiated in the 50s, has largely been based on an opposite conception of the Euler equations as being more accessible to computation than the

Navier-Stokes equations. Accordingly, the main interest has been focussed on inviscid equations, and a particular issue arising in this case, namely the existence of certain discontinuous solutions to the inviscid Euler equations for compressible flow corresponding to *shocks* or *contact discontinuities*. The analogous solutions of the viscous Navier-Stokes equations are smooth with layers replacing the discontinuities, of width decreasing with the viscosity. To mathematically handle such discontinuous solutions of the inviscid equations, the concept of *weak solutions* of (1) was introduced, defined using the conservation form allowing the derivatives to be applied to smooth test functions in a duality setting. It was then noted that certain discontinuous weak solutions have an unphysical nature, and *physically admissible weak solutions*, or *entropy solutions*, were identified as satisfying certain additional *entropy conditions* or *entropy inequalities* related to certain *entropy functions* of the solution. The entropy inequalities are automatically satisfied by smooth solutions, but not necessarily by discontinuous weak solutions. For scalar conservation laws, enough entropy functions are known to guarantee uniqueness, but for the inviscid Euler equations of compressible flow, essentially only one entropy function is known, the physical entropy, which does not appear to be enough to guarantee uniqueness. The question of existence and uniqueness of solutions of the inviscid Euler equations is therefore still unresolved, and it appears that the indicated traditional program based on weak solutions of the inviscid equations satisfying entropy conditions, can not be carried to the desired goal. Instead, it appears that Euler solutions (in three dimensions) in fact may be effectively uncomputable, and as already indicated it appears to be necessary to shift the focus to viscid forms of the equations, which may be expected to have unique solutions, albeit their complexity and the work to compute solutions in general may increase with decreasing viscosity. The increasing complexity requires turbulence modeling introducing viscous effects which reduce the complexity. The design of turbulence models is a main open problem, where today computational methods may offer new possibilitites.

A corresponding situation is met e.g. in elasto-plasticity, where the traditional model of perfect plasticity, which was motivated by its simplicity, in fact may be degenerate with non-unique solutions, which must be regularized by introducing viscous effects. The simplicity of the inviscid models were appealing in the early years of computing when computational power was very limited, and could then give useful information in certain very special cases, but with the massive computational power available today, it is natural to shift focus to more complete and non-degenerate viscid models.

The traditional computational methodology for conservation laws, with focus on the inviscid case, has been dominated by *finite difference methods* initiated in the 40s by Friedrichs and von Neumann and *finite volume methods* based on the work by Godunov in the 50's. The basic interest and work has been directed to the following topics:

- weak consistency
- entropy consistency

– shock capturing
– artificial viscosity
– a priori convergence results.

A computational method for a conservation law is *weakly consistent* if a limit of computed solutions as the mesh size tends to zero, is a weak solution of the conservation law. If the limit also satisfies the entropy conditions, then the method is *entropy consistent. Shock capturing* concerns oscillation-free (monotone) approximation of discontinuous solutions such as shocks or contact discontinuities. The traditional route to guarantee weak consistency is to use finite difference methods on so called *conservation form*, mimicing the form of the conservation law on uniform computational grids. The *artificial viscosity* is the effective viscosity used in the computation, which usually is nonzero even solving inviscid problems. Entropy consistency and monotone shock capturing may be guaranteed by introducing enough artificial viscosity, but too much will decrease the accuracy and produce smeared numerical layers. A basic problem is to find just the right amount of artificial viscosity to guarantee entropy consistency while keeping numerical layers as sharp as possible. A basic traditional result states that first order artificial viscosity (proportional to the mesh size) is enough, but too much because the resulting method is only first order accurate, and in particular contact discontinuities will be seriously smeared. The traditional convergence results based on the work of Kruzkov from the 60s are of a priori type proving typically convergence of first order schemes with first order artificial viscosity for scalar conservation laws using compactness and monotonicity methods. Very few a priori convergence results are available for systems of conservation laws (even in one space dimension), and/or higher order schemes, reflecting the lack of mathematical results on existence, uniqueness and stability of solutions, and generality of numerics.

Our work is based on *General Galerkin finite element methods*, referred to as G^2-methods, including *least squares stabilization*, *residual-based artificial viscosity*, and *space-time finite elements* as prime ingredients, which offer a rich spectrum of computational techniques with a common mathematical basis, and which may be applied to a large variety of differential equations, such as systems of conservation laws including models for compressible flow. The richness of this approach makes it possible to view many existing finite difference and finite volume methods as particular cases, but also opens entirely new possibilities of computational solution of conservation laws including in particular the goals of reliability and efficiency, which were not addressed in the traditional setting of finite difference and finite volume methods. We seek to realize these goals by using adaptive methods based on *a posteriori error estimates*, which take the following basic form:

$$\|u - U\| \leq S_c \|\frac{h^2}{\hat{\epsilon}} R(U)\|, \tag{3}$$

where the error $u - U$ in the given norm $\|\cdot\|$, e.g. an $L_p(L_q)$-norm in time-space, is estimated in terms of the mesh size $h = h(x)$, the artificial viscosity $\hat{\epsilon} = \hat{\epsilon}(U, x)$, the residual of the computed solution $R(U)$, and certain computable stability factors $S_c = S_c(u)$ defined through a continuous linearized dual problem and expressing relevant stability properties of the solution u being computed. The adaptive methods use

$$S_c \|\frac{h^2}{\hat{\epsilon}} R(U)\| \leq TOL \tag{4}$$

as *stopping criterion* guaranteeing the desired error control (2) through (3), and involve *modification strategies* aimed at realizing (4) at minimal computational cost, often based on *equi-distribution* of element contributions to the total error estimate. The *a priori* analog of (3) takes the basic form

$$\|u - U\| \leq S_{c,h} \|h^2 D^2 u\|, \tag{5}$$

where $S_{c,h}$ is an analog of S_c defined through a discrete dual problem, and D^2 denotes second derivatives in space. Conceptually, this estimate is obtained from (3) by using that $R(U) \approx \hat{\epsilon} D^2 U$ (including only the viscous term of the conservation law), and replacing U by u. The size of the stability factors S_c and $S_{c,h}$ of course is decisive for computability: if these factors are very large, then the solution u is uncomputable, while if they are of moderate size, then the computational work is comparable to that of direct interpolation of the solution u (if the solver is efficient with work proportional to the number of unknowns).

In the new setting of G^2-methods, the classical, largely unresolved, crucial questions concerning weak consistency, entropy consistency and the design of artificial viscosities, in particular for higher order methods for systems in several dimensions, may be given conclusive answers. For example, weak consistency is guaranteed simply by using Galerkin-type methods, and entropy consistency by requiring $\hat{\epsilon} \geq h^2 R(U)$, coupling the artificial viscosity to the residual $R(U)$ of the computed solution. Thus, the new approach offers not only answers to certain new questions of prime importance, but also offers new answers to some of the basic old questions. In the new setting, the quantity $\frac{h^2}{\hat{\epsilon}} R(U)$ obviously plays a key role.

We focus on the following issues in the setting of systems of conservation laws in several dimensions:

- design of G^2-methods: least squares modification, artificial viscosity, space-time meshes
- a posteriori error estimates, adaptive methods
- stability properties of the linearized equations, including computation of the stability factors S_c for bench-mark problems.

For maximal simplicity of presentation, we use the context of a scalar conservation law in one space dimension as much as possible, and present the extensions to systems of conservation laws in several dimensions more concisely. We first quickly review some basic facts concerning conservation laws, using the context of a scalar conservation law in one space dimension, including the basic types of solutions (shocks, and rarefactions), and the concepts of weak solution and entropy solution. This material overlaps some with the background material presented in the chapter by E. Tadmor, but the emphasis in this chapter is somewhat different because the numerics is different. We then turn to the main topic, the G^2-method, starting with the *characteristic Galerkin method*, we prove a posteriori error estimates of the form (3), and give theoretical information on the crucial stability issues in basic cases. We illustrate with new computational results from [3] focussing on the aspects of stability factors and dual solutions. We then extend the scope to the compressible Euler and Navier-Stokes equations. For additional numerical results using the adaptive methods, we refer to the references cited above.

2 Scalar conservation laws in one dimension

We start considering a scalar conservation law in one space dimension:

$$\begin{aligned} \dot{u} + (f(u))' - \epsilon u'' = 0, \quad x \in \mathbb{R},\ t > 0, \\ u(x,0) = u_0(x), \quad x \in \mathbb{R}, \end{aligned} \tag{6}$$

where the convective flux $f(u)$ is a given smooth function of u, u_0 is a given initial value, ϵ is a constant positive viscosity, $\dot{v} = \frac{\partial v}{\partial t}$ and $v' = \frac{\partial v}{\partial x}$. Since $(f(u))' = A(u)u'$, where $A = \frac{df}{du}$ denotes the derivative of f, the conservation law (6) can be written

$$\dot{u} + A(u)u' - \epsilon u'' = 0, \tag{7}$$

which has the form of a convection-diffusion equation $\dot{u} + \beta u' - \epsilon u'' = 0$, with the convection velocity $\beta(x,t) = A(u(x,t))$ depending on the solution $u = u(x,t)$.

We consider (6) posed on $\mathbb{R}$, and we also need to impose suitable boundary conditions at $x = \pm\infty$ for $t > 0$, such as the homogenous Dirichlet boundary condition $u(x,t) \to 0, x \to \pm\infty$. We may also pose the conservation law on a bounded interval, again with e.g. Dirichlet boundary conditions.

We focus mainly on the case with the viscosity ϵ being small, which offers the richest interaction between convective and diffusive fluxes $f(u)$ and $-\epsilon u'$, respectively. The *inviscid form* of (6) with $\epsilon = 0$, reads:

$$\begin{aligned} \dot{u} + (f(u))' = 0, \quad x \in \mathbb{R},\ t > 0, \\ u(x,0) = u_0(x), \quad x \in \mathbb{R}. \end{aligned} \tag{8}$$

For scalar problems in one space dimension, inviscid solutions are limits of viscid solutions as ϵ tends to zero, and may have a simple form in basic cases, including shocks, rarefactions and contact discontinuities. For systems in several dimensions, the complexity of solutions in general increases with decreasing ϵ, when eventually the flow becomes turbulent.

With $f(u) = u^2/2$, the problem (6) is referred to as *Burgers' equation*:

$$\dot{u} + uu' - \epsilon u'' = 0,$$

after the American mathematician Burgers, who used this model in a study of turbulence in fluid flow. We now present a similar basic flow model with $f(u) = u(1-u)$.

2.1 A model for traffic flow

We consider a model for traffic flow along a highway represented by $\mathbb{R}$, where $\rho(x,t)$ denotes the density ($0 \leq \rho \leq 1$) and $u(x,t)$ the velocity of cars at $x \in \mathbb{R}$ at time t. Conservation of mass, assuming that no cars enter or leave the highway, is expressed through the conservation law

$$\dot{\rho} + (u\rho)' = 0 \quad \text{in} \quad Q = \mathbb{R} \times (0,T), \tag{9}$$

which is complemented by a constitutive relation between u and ρ. A simple model is given by

$$u = 1 - \rho, \tag{10}$$

stating that the velocity varies linearly with the density from 1 if the road is empty, to zero if the road is packed. A more elaborate model is given by

$$u = 1 - \rho - \epsilon\rho'/\rho, \tag{11}$$

where $\epsilon > 0$, describing a driver who reduces speed if the density is increasing ahead, and vice versa. The simple model (10) is obtained setting $\epsilon = 0$. Combining (9) and (11), we obtain the following model for traffic flow

$$\dot{\rho} + ((1-\rho)\rho)' - \epsilon\rho'' = 0. \tag{12}$$

This equation is very similar to Burgers' equation and the above discussion directly applies. In particular, (12) also has shocks, corresponding to the sudden stops met in driving, and rarefaction waves corresponding to the gradual initiation of the traffic flow when a traffic light switches from red to green, see the figure below illustrating a situation with the red light at $x = 0$ turning green at $t = 0$.

An unphysical discontinuous solution in the case $\epsilon = 0$, corresponds to the situation when the driver closest to the traffic light looking in his rear mirror notices that the density of cars is equal to one behind, and therefore decides to maintain zero speed even when the traffic light changes to green. One may say that this corresponds to a *stupid driver* who does not understand the entropy inequality, while the model (11) corresponds to an *intelligent driver* who will respect this condition, and thus in particular will get started as the first car at the switch to green.

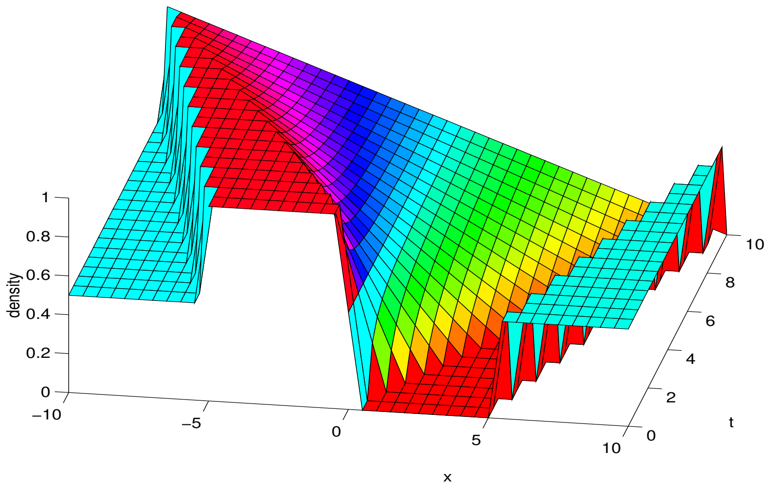

We note that the unphysical solution is unstable: even a very slight "honk" should make the stupid driver aware of the green traffic light and make him get started into a rarefaction, which is very different from the unphysical solution after some time. The physical solution on the other hand is stable: a small perturbation of initial data will not change the solution dramatically. This is another aspect of the entropy condition characterizing physical solutions: Weak solutions which do not respect the entropy condition, may be unstable to very small disturbances, which give them an "unphysical" nature. We will return below to aspects of stability of shocks and rarefactions.

2.2 The Euler equations for a compressible inviscid perfect gas

The Euler equations in one dimension for a compressible inviscid perfect gas in conservation variables (ρ, m, e), take the form of the following system of conservations laws

$$\begin{aligned} \dot\rho + (u\rho)' &= 0, \quad x\in\mathbb{R},\ t>0,\\ \dot m + (um)' + p' &= 0, \quad x\in\mathbb{R},\ t>0,\\ \dot e + (ue)' + (pu)' &= 0, \quad x\in\mathbb{R},\ t>0, \end{aligned} \tag{13}$$

together with boundary and initial conditions, where ρ is the density, $m=\rho u$ the momentum density with u the velocity, e the energy density, and p the pressure given by the perfect gas law $p=(\gamma-1)(e-m^2/(2\rho))$, where $\gamma>1$ is a constant. The equations express conservation of mass, momentum and energy, where the momentum equation corresponds to Newton's law with p' representing the net force density on a fluid element from the pressure, and in the energy equation $(pu)'$ represents the work density from the pressure acting on a fluid element. Here $u\rho$, um and ue are the convective fluxes of the mass, momentum and energy, and p' and $(pu)'$ are fluxes related to the pressure.

The physical entropy η is given by $\eta = -\rho \log(p\rho^{-\gamma})$ with corresponding entropy flux $u\eta$.

2.3 Characteristics

We may attempt to solve the inviscid conservation law (8) using the *method of characteristics*, and in particular we could hope this way to obtain approximate solutions of the viscid equation (6) if ϵ is small. The *characteristics* of (8) are curves $x = x(\bar{x}, \bar{t})$, such that

$$\frac{dx}{d\bar{t}} = A(u(x, \bar{t})), \text{ for } \bar{t} > 0, \quad x(\bar{x}, 0) = \bar{x},$$

where u is a differentiable solution of (8) satisfying $\dot{u} + A(u)u' = 0$. Since by the chain rule,

$$\frac{d}{d\bar{t}} u(x(\bar{x}, \bar{t}), \bar{t}) = \frac{du}{dx}\frac{dx}{d\bar{t}} + \frac{du}{d\bar{t}} = A(u)u' + \dot{u} = 0, \ \bar{t} > 0,$$

it follows that u is constant along a characteristic. Thus, $\frac{dx}{dt}$ is also constant along a characteristic, which therefore must be a straight line. This means that the solution of (8) is obtained by drawing from each point $(\bar{x}, 0)$ a straight line with slope $A(u_0(\bar{x}))$ and noting that the solution u is constant equal to $u_0(\bar{x})$ along that line. We may express the nature of the solution of (8) by stating that the level curves of a solution are straight lines coinciding with characteristics. This solution method works as longs as characteristics do not cross.

Considering now for definiteness the case of Burgers' equation with $A(u) = u$, we next note that if u_0 is decreasing, then two charateristics starting at two distinct points $\bar{x}_1$ and $\bar{x}_2$ may actually cross for $\bar{t} > 0$, and then we have the conflicting statement that u at the intersection should have both the value $u_0(\bar{x}_1)$ and $u_0(\bar{x}_2)$, which are different. We shall see that this corresponds to the formation of a shock wave, which is a discontinuous solution corresponding to a propagating sharp front. The "bang" from a supersonic airplane, or the "bang" in the water pipe system of a house from closing a faucet, are examples of shock waves.

2.4 Basic solutions: rarefaction and shock waves

We now recall the basic types of solutions in the context of the inviscid Burgers' equation. We have seen that if u_0 is increasing and continuous, then the method of characteristics works, and we obtain a continuous solution. If u_0 is increasing and discontinuous, with two constant states in the basic case, then the method of characteristics can be extended to give a solution referred to as a *rarefaction wave*, which is a continuous solution connecting at each time level the two constant states by a linear transition of width proportional to $t > 0$. We give the details shortly. If u_0 is decreasing and discontinuous with two constant states, then the corresponding solution is a shock wave consisting of two constant states for all $t > 0$. A shock may also develop after some time starting with decreasing continuous data. This corresponds to the development of a breaking wave on a shore. We now consider the case of rarefaction wave and shock wave separately in more detail.

Rarefaction wave Consider the inviscid Burgers' equation with the increasing discontinuous initial data $u_0(x) = 0$ for $x < 0$, and $u_0(x) = 1$ for $x > 0$. The exact solution is the rarefaction wave given by

$$\begin{array}{lll} u(x,t) = 0 & \text{for} & x < 0, \\ u(x,t) = \frac{x}{t} & \text{for} & 0 \leq \frac{x}{t} \leq 1, \\ u(x,t) = 1 & \text{for} & 1 < \frac{x}{t}. \end{array} \tag{14}$$

This is a continuous function for $t > 0$, differentiable off the lines $x = 0$ and $x = t$, which satisfies (8) in fact for all (x,t) for $t > 0$, and thus is a solution in a classical sense. In a rarefaction wave, an initial discontinuity separating two constant states develops into a continuous linear transition from one state to the other of width t in space, corresponding to "fan-like" level curves in space-time, see below. The solution may be found using the method of characteristics for $x < 0$ and $1 < \frac{x}{t}$ and is completed with the fan-like transition which gives a solution which is continuous for $t > 0$.

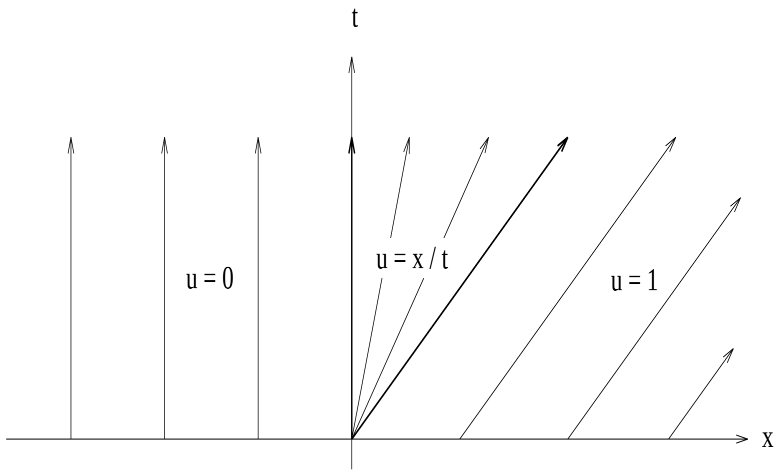

Shock We consider now the decreasing discontinuous initial data $u_0(x) = 1$ for $x < 0$, and $u_0(x) = 0$ for $x > 0$. The limit of solutions of the viscid Burgers' equation as ϵ tends to zero, turns out to be the following discontinuous function corresponding to a shock wave moving with speed $\frac{1}{2}$,

$$\begin{aligned} u(x,t) &= 1 \quad \text{for} \quad x < \tfrac{t}{2}, \\ u(x,t) &= 0 \quad \text{for} \quad x > \tfrac{t}{2}. \end{aligned} \tag{15}$$

The corresponding solutions for $\epsilon > 0$ are smooth approximations of the discontinuity of width ϵ, with u' being negative and of size ϵ^{-1} in the transition zone from 1 to 0.

In the present case the initial discontinuity is maintained, in contrast to the above case of a rarefaction wave, where the initial discontinuity is turned into a continuous linear transition from one state to the other over a distance in space of length t. The method of characteristics breaks down in the shock wave case with the two characteristics at the two sides of the shock with slopes 1 and 0 respectively, converging into the shock with slope 1/2, see below.

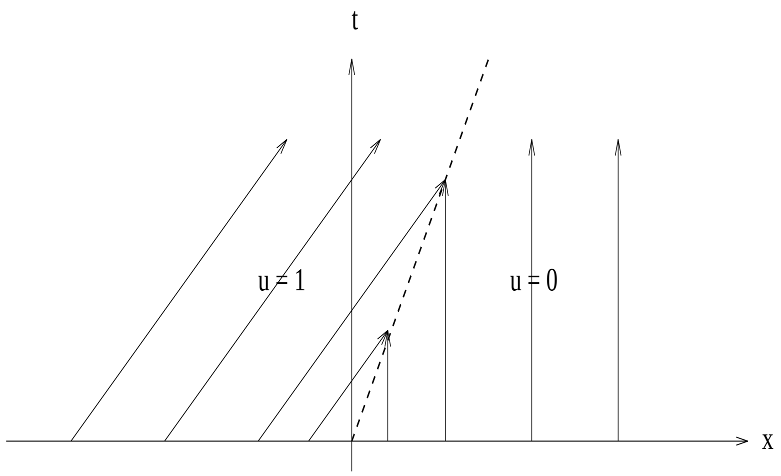

2.5 Weak solutions and the Rankine-Hugoniot condition

We say that the bounded function $u(x,t)$ is a *weak solution* of the equation $\dot{u} + (f(u))' = 0$ for $x \in \mathbb{R}$ and $t > 0$ if for all smooth functions $\varphi(x,t)$ which vanish for $t = 0$ and for $|x| + t$ large,

$$\int_{\mathbb{R}} \int_0^\infty -(u\dot{\varphi} + f(u)\varphi')dx\,dt = 0. \tag{16}$$

This relation is formally obtained multiplying $\dot{u} + (f(u))' = 0$ by φ and integrating by parts putting the derivatives on φ. Note that by the vanishing of φ, no boundary terms arise from from the integration by parts. The concept of weak solution is the minimal requirement we can put on a function to satisfy the conservation law $\dot{u} + (f(u))' = 0$. This is analogous to the variational (or weak formulation) of the Poisson equation, where "half" of the derivatives are put on the test functions. In the present case we go one step further and put all derivatives on the test function φ. It is the conservation form of the equation which makes this possible.

Let us thus seek to find a discontinuous weak solution $u(x,t)$ defined by $u(x,t) = u_+$ if $x > st$ and $u(x,t) = u_-$ if $x < st$, where u_+ and u_- are two constant states, and s is a constant, corresponding to a discontinuity propagating with speed s. Inserting this function into (16) and integrating by parts gives

$$\int_\Gamma ([u]n_t + [f(u)]n_x)\varphi ds = 0,$$

where Γ is the straight line $\{(x,t) : x = st, t \geq 0\}$ with normal (n_x, n_t) parallel to $(-1, s)$, and $[u] = u^+ - u^-$ and $[f(u)] = f(u^+) - f(u^-)$ are the jumps of u and $f(u)$ across Γ. Since $s = -n_t/n_x$ this gives the following relation, referred to as the *Rankine-Hugoniot condition*, relating the shock speed s to the jumps in u and $f(u)$:

$$s = \frac{[f(u)]}{[u]}. \tag{17}$$

For Burgers' equation with $f(u) = u^2/2$, we have

$$s = (u_+ + u_-)/2. \tag{18}$$

In the above example, we thus find that $s = \frac{1}{2}$. The Rankine-Hugoniot condition expresses the conservation of the quantity u expressed in the conservation law $\dot{u} + (f(u))' = 0$ in the case of a discontinuous solution.

2.6 Weak solutions may be non-unique

Consider the inviscid Burgers' equation with the rarefaction wave initial data $u_0(x) = 0$ for $x < 0$ and $u_0(x) = 1$ for $x > 0$. The function

$$\begin{aligned} u(x,t) = 0 \quad &\text{for} \quad x < \tfrac{t}{2}, \\ u(x,t) = 1 \quad &\text{for} \quad x > \tfrac{t}{2}, \end{aligned} \tag{19}$$

is a weak solution, with a discontinuity $\{x,t) : x = st\}$ moving with speed $s = \frac{1}{2}$. However, this solution is different from the rarefaction wave solution (14), which since it is a classical solution, also is a weak solution. Thus, we have in this case two different weak solutions, and thus we have an example of non-uniqueness of weak solutions. From a physical point of view, only the rarefaction wave solution is an acceptable solution. This is because the function (19) does not satisfy certain entropy inequalities, which characterize physically admissible weak solutions, while the rarefaction wave solution does so. On the other hand, the discontinuous shock wave solution does satisfy the entropy inequalities, and thus the shock is a physically admissible solution. We now turn to a discussion of the entropy inequalities satisfied by physically admissible solutions.

We have already remarked that exact solutions of the viscous conservation law always do satisfy the entropy inequalities, while weak solutions of the inviscid law may fail to do so. This turns out to be of mayor concern for the design of numerical methods for conservation laws in the case of small viscosity. In fact, to guarantee that approximate numerical solutions properly satisfy the entropy inequalities, which is necessary to avoid that the numerical solution seeks to approximate a non-physical solution, the numerical method must effectivly introduce a sufficient amount of numerical or "artificial" viscosity. This is because the given viscosity may be too small compared to the mesh size used to guarantee satisfaction of the entropy inequalities. A basic problem in the design of numerical methods for conservation laws with small viscosity, is thus the design of the artificial viscosity of the numerical method. We present below a solution to this basic problem, which generalizes to systems of conservation laws.

2.7 Entropy inequalities

The entropy inequalities are related to the Second Law of Thermodynamics stating that in a closed physical system, the entropy cannot decrease. Intuitively, the physical concept of "entropy" is related to "disorder" or "loss of information" and thus the The Second Law states that disorder cannot decrease. To see how the Second Law in this form applies to the shock wave case above, we note that the characteristics in this case "converge into" the shock, which may be viewed as a "loss of information", or increase of entropy, which is physically admissible. On the other hand, for the unphysical solution (19), the characteristics seem to "emerge from" the discontinuity, which may be viewed as some kind of "creation of information", which would contradict the Second Law. Thus, in brief we may say that a discontinuous weak solution with the characteristics converging into the discontinuity, is a physical solution while it is unphysical if the characteristics are divering out from the discontinuity.

Let us now turn to the entropy inequalitites which express the Second Law in quantitative analytical form. For definiteness we consider Burgers' equation in viscid form. We first notice that multiplying by u, integrating in time and space, we obtain the following basic energy estimate:

$$\int_{\mathbb{R}} |u(x,t)|^2\,dx + D_\epsilon(u) = \int_{\mathbb{R}} |u(x,0)|^2\,dx, \tag{20}$$

where

$$D_\epsilon(u) = 2\int_0^t \int_{\mathbb{R}} \epsilon(u')^2\,dx\,ds. \tag{21}$$

In particular, it follows that for $t > 0$

$$\|u(\cdot,t)\| \leq \|u_0\|, \tag{22}$$

with $\|\cdot\|$ denoting the $L_2(\mathbb{R})$-norm.

We now compare the size of $D_\epsilon(u)$ in the case of a rarefaction wave and a shock wave. We find that $D_\epsilon(u) \propto \epsilon$ in the case of a rarefaction wave and $D_\epsilon(u) \propto [u]$ in the case of a shock wave with jump $[u]$. Thus, in the rarefaction wave case $D_\epsilon(u) \to 0$ as $\epsilon \to 0$, while in the shock case we have $D_\epsilon(u) \to [u] \neq 0$ as $\epsilon \to 0$. Thus, we will have equality in (22) in the case of a rarefaction wave, and strict inequality in the case of a shock wave. This may be viewed as expressing a "loss of information" or "entropy production" in the case of a shock wave.

We now present a sharper variant of the preceeding analysis with the aim of connecting to the above discussion of the direction of characteristics at a shock. We then assume that the solutions u of the viscid Burgers' equation u are bounded for $\epsilon > 0$, and tend pointwise to some bounded limit, again denoted by u, as ϵ tends to zero. Multiplying Burgers' equation first by smooth test function φ with compact support (vanishing for $t = 0$ and $t + |x|$ large), and integrating by parts, we obtain

$$\begin{aligned} -\textstyle\int_0^t \int_{\mathbb{R}} u\dot\varphi\,dx\,ds - \frac{1}{2}\int_0^t \int_{\mathbb{R}} u^2\varphi'\,dx\,ds \\ = -\textstyle\int_0^t \int_{\mathbb{R}} \epsilon u'\varphi'\,dx\,ds. \end{aligned}$$

Since by (20)

$$2\int_0^t \int_{\mathbb{R}} \epsilon(u')^2\,dx\,ds \leq \|u_0\|^2, \tag{23}$$

we have using Cauchy's inequality and the smoothness of φ,

$$\int_0^t \int_{\mathbb{R}} \epsilon u'\varphi'\,dx\,ds \leq \|u_0\|\sqrt{\epsilon}(\int_0^t (\varphi')^2 dx\,ds)^{1/2} \to 0 \quad \text{as } \epsilon \to 0. \tag{24}$$

Thus, we conclude that the limit u satisfies (16) with $f(u) = u^2/2$ and hence is a weak solution of the inviscid Burgers' equation.

Next, multiplying by $u\varphi$, where φ is a smooth function with compact support, now assumed to be also non-negative, we obtain integrating by parts

$$\begin{aligned} -\textstyle\int_0^t \int_{\mathbb{R}} \frac{u^2}{2}\dot\varphi\,dx\,ds - \int_0^t \int_{\mathbb{R}} \frac{u^3}{3}\varphi'\,dx\,ds \\ +\textstyle\int_0^t \int_{\mathbb{R}} \epsilon(u')^2\varphi\,dx\,ds = -\int_0^t \int_{\mathbb{R}} \epsilon u u'\varphi'\,dx\,ds. \end{aligned}$$

Arguing as above, using also the boundedness of u, we see that the right hand side tends to zero. Using also the positivity of φ to see that the third term on the right hand side is positive, we conclude that the limit u satisfies

$$-\int_0^t \int_{\mathbb{R}} \frac{u^2}{2}\dot\varphi\,dx\,ds - \int_0^t \int_{\mathbb{R}} \frac{u^3}{3}\varphi'\,dx\,ds \leq 0, \tag{25}$$

for all smooth non-negative functions φ with compact support, with strict inequality if $D_\epsilon(u)$ tends to some non-zero limit. This is an entropy inequality stated in weak form, with the derivatives on the test function φ. In strong form obtained formally integrating by parts and using the positivity of φ, the entropy inequality may be stated

$$\frac{d}{dt}(\frac{-u^2}{2}) + \frac{d}{dx}(\frac{-u^3}{3}) \geq 0, \tag{26}$$

For smooth solutions of the inviscid Burgers' equation $\dot{u} + uu' = 0$, this relation is obtained (with equality) simply by multiplying by u and integrating. The above derivation shows that a limit of solutions of the viscid Burgers' equation, satisfies this relation, possibly with strict inequality (e.g. in the case of a shock). Integrating (26) in space and time with homogenous Dirichlet boundary conditions, in which case the x-derivative term integrates to zero, we obtain a global form of the entropy inequality which coincides with the basic L_2 estimate (22). In the present case the entropy of u is equal to $-u^2/2$.

Suppose now that the limit u is discontinuous with two states separated by the line $x = st$: $u(x,t) = u_-$ for $x < st$ and $u(x,t)$ for $x > st$. The Rankine-Hugoniot condition (18) expressing that this function is a weak solution, is $s = \frac{1}{2}(u_- + u_+)$. Inserting next the function u into the entropy inequality (25), and using partial integration as in the derivation of the Rankine-Hugoniot condition, we find that

$$s[\frac{u^2}{2}] - [\frac{u^3}{3}] \geq 0. \tag{27}$$

We thus find by a simple computation that

$$0 \leq \frac{1}{2}(u_- + u_+)\frac{1}{2}[u^2] - \frac{1}{3}[u^3] = (u_- - u_+)\frac{1}{12}(u_- - u_+)^2. \tag{28}$$

We conclude that the entropy inequality in this case may be stated $u_- \geq u_+$, or equivalently,

$$u_- \geq s \geq u_+. \tag{29}$$

This version of the entropy inequality states that the characteristics of a physically admissible discontinuous weak solution of the inviscid Burgers equation "converge into" the shock.

2.8 General convex entropies

We will refer to $\eta(u) = \frac{u^2}{2}$ as the "mathematial entropy" of u corresponding to the "physical entropy" $-\frac{u^2}{2}$ under consideration, the difference being the sign. The global form of the entropy inequality, which coincides with the basic L_2-estimate (22), may then be stated

$$\int_{\mathbb{R}} \eta(u(x,t))dx \leq \int_{\mathbb{R}} \eta(u(x,0))dx, \quad \text{for } t > 0, \tag{30}$$

Below, we will work with the concept of mathematical entropy, following the tradition in the mathematical literature on conservation laws, and simply refer to this concept as entropy. With this terminology, the Second Law states that the entropy cannot increase.

More generally, for scalar conservation laws any convex function $\eta(u)$, may be used as an *entropy*. The function $\eta(u) = u^2/2$ is then the basic example of an entropy. Arguing as above multiplying (6) by $\eta'(u)\varphi$, and using that $\eta'' \geq 0$, we obtain the following entropy inequality stated in strong form

$$\frac{\partial}{\partial t}(\eta(u)) + \frac{\partial}{\partial x}(q(u)) \leq 0, \tag{31}$$

where $q(u)$ is the *entropy flux* satisfying the compatibility condition

$$q' = f'\eta'. \tag{32}$$

We note that in the present case, we may find for any choice of $\eta(u)$, an entropy flux $q(u)$ satisfying the compatibility condition (32), and as a consequence we obtain a family of entropy inequalites corresponding to the family of convex functions $\eta(u)$. This means that a physically admissible solution in the present scalar case satisfies (31) for a whole family of different entropies. A basic mathematical result for scalar conservation laws guarantess uniqueness of weak solutions satisfying all the entropy inequalities related to convex entropies.

For the system of conservation laws modeling inviscid compressible flow the situation is different: in this case only one entropy is known (up to simple modifications corresponding to adding a constant and multiplying by a constant), which is the one physical entropy given by Nature. It is not known if the corresponding single entropy inequality is enough to guarantee uniqueness of weak solutions. Accordingly, the mathematical theory for systems of inviscid conservation laws remains severely incomplete.

To sum up, we have shown that a limit of viscous solutions of (6), as ϵ tends to zero, satisfies the entropy inequality (31) for any convex entropy $\eta(u)$. A basic problem in the analysis of numerical methods will be to establish the same property for limits of numerical solutions. We shall see below that the basic mechanism to build this property into the numerical method, is to add enough artificial viscosity. On the other hand, from accuracy point of view we should not use more artificial viscosity than necessary. A basic problem is thus to find the minimal amount of artificial viscosity needed to guarantee the proper satisfaction of the entropy inequalities. We will present a solution to this problem below.

3 G^2: Generalized Galerkin methods

We now turn to the G^2-method based on Galerkin's method combined with (i) weighted least-squares modification, (ii) residual-based artificial viscosity and (iii) space-time piecewise polynomial approximation. The G^2-method offers a rich spectrum of computational methods depending on the choice of the space-time mesh. These methods may be classified as *Eulerian* with the space-time mesh oriented along the space and time coordinate axis, *Lagrangean* with the space-time mesh oriented along particle paths in space-time, and Arbitrary Lagrangean-Eulerian or *ALE* methods with the space-time mesh oriented according to some other feature such as space-time gradients of the solution. We also refer to Lagrangean variants as *characteristic Galerkin* or chG-methods, or more precisely as chG(p,q)-methods with piecewise polynomials of order p in space, and piecewise polynomials of order q along space-time particle paths, and similarly to ALE-methods with the space-time mesh oriented according to space-time gradients of the solution as *oriented Galerkin* orG(p,q)-methods. We also refer to the Eulerian variants as *Streamline diffusion*, or Sd-methods. In all these variants the space-time mesh is usually organized in *space-time slabs* between discrete time levels, and the space mesh may be changed across the discrete time levels to avoid mesh distortion and allow mesh adaption. When the space mesh is changed across a discrete time level, a *projection* from the previous mesh to the new mesh at that time level, is performed. The projection is built into the Galerkin method through a jump term and corresponds to a modified L_2 projection with a residual-based artificial viscosity. The discrete solution between the discrete time levels may be viewed as an approximate *transport* step, and the whole process may be viewed as a method of the basic form *projection-transport*.

The traditional finite difference methods are of Eulerian type with the first order Lax-Friedrichs' scheme from the 50s as a prototype on conservation form and with artificial viscosity proportional to the mesh size. The next generation of classical schemes originates from Godunov's method in 1d, which is of the form projection-transport with piecewise constant (discontinuous) approximation and a Riemann solver for the transport step. The multi-dimensional finite volume schemes developed in recent decades, use discontinuous polynomial approximation with numerical fluxes often constructed using 1d Riemann solvers. These methods may alternatively be viewed as particular G^2 methods with discontinuous piecewise polynomials, or *discontinuous Galerkin* or dG-methods.

An outline of the remainder of this chapter is as follows: We first present the chG(1,0) method, continue with an Eulerian Sd-method, which we refer to as cG(1)dG(0) with continuous piecewise linears in space and discontinuous piecewise constants in time. We also present a full dG(q)-method, based on discontinuous piecewise polynomial approximation in space-time of degree q. We start with scalar conservation laws in 1d, and conclude with the multi-d systems given by the Euler and Navier-Stokes equations for compressible flow. We present in particular computations of dual solutions and stability factors.

3.1 The characteristic Galerkin method chG(1,0)

For the numerical solution of the conservation law (6), we now consider the characteristic Galerkin method chG(1,0), which is the particular variant of the General Galerkin G^2-method with the space-time mesh oriented according to characteristics, and with piecewise linear approximation in space and piecewise constant approximation along characteristics. We complement (6) with homogenous Dirichlet boundary conditions, assuming that $u_0(x)$ vanishes for $|x|$ large.

To define chG(1,0), let $0 = t_0 < t_1 < ...$, be an increasing sequence of time levels, let $S_n = \mathbb{R} \times I_n$ where $I_n = (t_{n-1}, t_n)$, be the corresponding space-time slabs. Associate to each slab S_n a set V_n of continuous piecewise linear functions on $\mathbb{R}$ with mesh function $h_n(x)$, and assume that the functions in V_n vanish for $|x|$ large. For a given velocity β defined on S_n, let

$$W_{kn}^{\beta} = \{v \in \mathcal{C}(S_n) : \dot{v} + \beta v' = 0 \quad \text{in } S_n, \quad v_{n-1}^{+} \in V_n\}, \tag{33}$$

where $\mathcal{C}(S_n)$ is the set of continuous functions on S_n, and

$$v_{n-1}^{+}(x) = \lim_{s \to 0^+} v(x, t_{n-1} + s).$$

Finally, set $W_k^{\beta} = \prod_n W_{kn}^{\beta}$. A function v in W_k^{β} is constant along the characteristics on each slab S_n defined by the mesh tilting velocity β, is in general discontinuous in time across the discrete time levels t_n, and the limit from above v_{n-1}^{+} at the initial time level t_{n-1} of each slab S_n is a piecewise linear function in V_n. To guarantee existence of the characteristics, we assume that β is Lipschitz continuous in x, and that the time step $k_n = t_n - t_{n-1}$ is sufficiently small. Below we shall see that it is natural to require that $\bar{h}_n^2/k_n$ tends to zero as $\bar{h}_n$ tends to zero, where $\bar{h}_n$ is the maximum of $h_n(x)$, which requires k_n not to be too small. Normally, the condition on k_n to avoid intersection of characteristics, is of the form $k_n \leq Ch_n(x)$, so that no conflict arises.

The chG(1,0) method for (6) may now be formulated as follows: find $U \in W_k^{\beta}$, where $\beta = A(U)$, such that for $n = 1, 2, ..., \forall v \in W_{kn}^{\beta}$,

$$(\dot{U} + A(U)U', v)_n + (\hat{\epsilon}\nabla U, \nabla v)_n + ([U_{n-1}], v_{n-1}^{+}) = 0, \tag{34}$$

where $[U_{n-1}] = U_{n-1}^{+} - U_{n-1}^{-}$ is the jump at time t_{n-1} with $v_{n-1}^{-}(x) = \lim_{s \to 0^+} v(x, t_{n-1} - s)$ the limit from below,

$$\hat{\epsilon} = \max(\epsilon, \gamma_1 h^{2-\kappa} R(U), \gamma_2 h^{\frac{3}{2}}), \tag{35}$$

$(\cdot,\cdot)_n = (\cdot,\cdot)_{L_2(S_n)}$, $R(U) = |[U_{n-1}]|/k_n$ on S_n (extended from t_{n-1} to S_n as constant in time), the γ_i are positive constants of moderate size, and κ is a small positive constant. This method can also be applied to the inviscid form (8) of (6) simply be setting $\epsilon = 0$ in the definition of $\hat{\epsilon}$.

The artificial viscosity $\hat{\epsilon}$ defined by (35) has the same form as that used in [5] for linear convection-diffusion problems. Roughly speaking, $\hat{\epsilon}$ may be viewed to be designed to guarantee that limits of chG(1,0)-solutions satisfy all entropy inequalities, while being as small as possible in order to maintain high accuracy. The crucial design feature is that

$$\frac{h^2 R(U)}{\hat{\epsilon}} \le h^\kappa/\gamma_1 \to 0 \quad \text{as } \bar{h} \to 0 \tag{36}$$

where $\bar{h} = \max_n \bar{h}_n$, the mathematical justification of which we present below. The artificial vicosity $\hat{\epsilon}$ defined by (35) is locally much smaller than the *classical artificial viscosity* of the simple form $\hat{\epsilon} \sim h$, which is the artificial viscosity of the Lax-Friedrichs' scheme, and which degrades the accuracy to first order everywhere. In a shock, $\hat{\epsilon}$ defined by (35) may be of order h, because there R may be of size $1/h$, but elsewhere $\hat{\epsilon}$ will be smaller, and the accuracy is improved.

By a fixed point argument one can prove that the nonlinear problem (34) for a given n, has solution if the time step k_n is so small that intersection of characteristics is avoided. Notice that the mesh tilting velocity $A(U)$ depends on the solution U. Notice further that the basic energy estimate for U implies that $|U'| \le C\hat{\epsilon}^{-1}$, which guarantees that the time steps do not have to be chosen smaller than $\hat{\epsilon}$.

Since by the construction, $\dot{U} + A(U)U' = 0$ on each slab S_n, the chG(1,0) method (34) reduces to finding $U \in W_k^\beta$ with $\beta = A(U)$, such that for $n = 1, 2, ...,$

$$(U_{n-1}^+, v_{n-1}^+) + (\hat{\epsilon}U', v')_n = (U_{n-1}^-, v_{n-1}^+) \quad \forall v \in W_{kn}^\beta. \tag{37}$$

This method may be viewed to be of the form "projection + transport". To see this, we may consider the following variant with the diffusion term acting on the discrete time level t_{n-1}, instead of the slab S_n: find $U \in W_k^\beta$ with $\beta = A(U)$, such that for $n = 1, 2, ...,,$

$$(U_{n-1}^+, v) + (\hat{\epsilon}U', v')_n^+ k_n = (U_{n-1}^-, v), \quad \forall v \in V_n, \tag{38}$$

where we use the notation

$$(v, w)_n^+ = \int_{\mathbb{R}} v_{n-1}^+ w_{n-1}^+ \, dx,$$

and a factor k_n came from the change of integration from S_n to $\mathbb{R}$. This method may be formulated as finding for $n = 1, 2, ..,$ the function $U_n \equiv U_n^-$, such that

$$U_n = T_n \tilde{P}_n U_{n-1}, \tag{39}$$

where $\tilde{P}_n$ is a modified $L_2(\mathbb{R})$ projection into V_n with artificial viscosity, defined by

$$(\tilde{P}_n w, v) + (\hat{\epsilon}(\tilde{P}_n w)', v')k_n = (w, v), \quad \forall v \in V_n, \tag{40}$$

where $\hat{\epsilon} = \max(\epsilon, \gamma_1 h^{2-\kappa}|w - \tilde{P}_n w|/k_n, \gamma_2 h^{\frac{3}{2}})$, and $T_n w$ is the solution at time t_n of the inviscid equation $\dot{u} + A(u)u' = 0$ on the slab S_n, with given initial data equal to w at time t_{n-1}. Other variants of this method are obtained by choosing different projections, and more generally using approximations of the transport step.

A very simple variant of (38) is obtained using the same uniform mesh underlying all V_n, and using a lumped mass $L_2(\mathbb{R})$ projection, see [4]. This method efficively adds classical artificial viscosity of order h from the lumping of the mass matrix in the projection performed at each time step, which dominates the artificial viscosity $\hat{\epsilon}$ given by (35). The simplified method may be summarized as: on time level t_{n-1}, compute $U_{n-1}^+ \in V_n$ at the nodes, as a mean value of U_{n-1}^- weighted with the proper hat function. Then solve the equation $\dot{u} + A(u)u' = 0$ on the slab S_n with initial data U_{n-1}^+ at time t_{n-1} using the method of characteristics, drawing from each node of T_n a line with slope $A(U_{n-1}^+)$, to get the solution U_n^-, and repeat. The artificial viscosity from the lumped L_2 projection is quite a bit of over-kill, and thus the accuracy of the lumped version is not as good as that of the more elaborate chG(1,0) method with the residual dependent artificial viscosity $\hat{\epsilon}$.

Following [4], we can genetralize chG(1,0) to chG(q,r) basing V_n on continuous piecewise polynomials of order q, and using discontinuous piecewise polynomial approximation of order r along characteristics.

3.2 The Sd-method

Choosing the mesh tilting velocity $\beta = 0$ and stabilizing using a weighted least squares modification, we obtain the following Eulerian variant, which we refer to as the cG(1)dG(0) Sd-method or Sd(1,0): find $U \in W_k^0$, such that for $n = 1, 2, ..., \forall v \in W_{kn}^0$,

$$(\dot{U} + A(U)U', v + \delta(\dot{v} + A(U)v'))_n + (\hat{\epsilon}\nabla U, \nabla v)_n + ([U_{n-1}], v_{n-1}^+) = 0, \quad (41)$$

where

$$\delta = \frac{1}{2}(k_n^{-2} + h_n^{-2} A(U)^2)^{-1/2},$$

$\hat{\epsilon} = \max(\epsilon, \gamma_1 h^{2-\kappa} R(U), \gamma_2 h^{\frac{3}{2}})$, and now $R(U) = |\dot{U} + A(U)U'| + |[U_{n-1}]|/k_n$ on S_n. The accuracy of this method is inferior to that of chG(1,0), because of the piecewise constant approximation in time, which does not in general fit with the solution feature of being constant along space-time characteristics. In particular, the Sd-method with piecewise constants in time, introduces artificial viscosity of order h, through the δ term. This method can directly be generalized to Sd(q,r)-methods based on cG(q)dG(r), which have higher accuracy and less viscosity, but are more computationally intensive.

3.3 The oriented Galerkin method

Orienting the mesh in the Sd-method (41) along characteristics replacing W_k^0 by $W_k^{A(U)}$, we have effectively $\dot{v} + A(U)v' = 0$ for $v \in W_k^{A(U)}$, so that we may choose $\delta = 0$, and thus the Sd(q,r)-method with the mesh orientation along characteristics, reduces to chG(q,r).

One can also choose the mesh tilting velocity β according to some other principle than following characteristics or setting $\beta = 0$. For example, one may seek to orient β to be perpendicular to the space-time gradient of the solution, with the direction of piecewise constant approximation along space-time level curves. This gives a different orientation of the mesh at shocks, which are propagated at a speed different from that of the two converging characteristics at the shock. We refer to such a method as an oriented Galerkin method (orG-method).

3.4 An analysis of chG(1,0)

We will analyze chG(1,0) in the form (38) through the following sequence of steps. We start with the inviscid case with $\epsilon = 0$. We first show that if a bounded sequence of chG(1,0)-solutions $\{U\}$ converges pointwise to a limit function u as the mesh size h tends to zero, then the limit u is (i) a weak solution, (ii) satisfies all entropy inequalities, that is, we prove (i) weak consistency and (ii) entropy consistency. By the uniqueness of a weak solution satisfying all entropy inequalities in the present scalar case, we thus can assure that a limit of chG(1,0)-solutions must be equal to the exact solution. Next, we prove L_2 a posteriori error estimates of the form (45), and we also indicate how to turn this estimate into an a priori estimate using an energy norm stability estimate to give the needed a priori information on the regularity of the chG(1,0) solution. Finally, we derive analytical estimates of the stability factors for the dual linearized problems in model cases associated to smooth solutions, shocks and rarefactions, showing that these factors are of moderate size. We conclude that the basic types of solutions of scalar conservation laws are computable in L_2 norms with essentially optimal work compared to interpolation.

We will assume below that the quantity $\alpha \equiv \max_n \bar{h}_n^2/k_n$ tends to zero as $\bar{h}$ tends to zero. This requires the time steps k_n not to be too small, but is not in conflict with the requirement of choosing sufficiently small time steps in order to avoid crossing of characteristics.

A basic energy stability estimate Choosing $v = U$ in 38, integrating by parts and summing over n, we obtain the following familiar basic energy estimate for $N \geq 1$,

$$\|U_N^-\|^2 + \sum_{n=1}^{N} \|[U_{n-1}]\|^2 + 2\sum_{n=1}^{N} (\hat{\epsilon} U', U')_n^+ k_n \leq \|u_0\|^2. \tag{42}$$

A limit of chG(1,0)-solutions is a weak solution To prove that a pointwise limit of a bounded sequence of chG-solutions $\{U\}$, is a weak solution of

(8), we let φ be an arbitrary smooth test function with compact support and choose in (38) the function $v = \pi_h\varphi \in W^\beta_{kn}$ to interpolate φ_{n-1} at the nodes of V_n. Integrating by parts, replacing v by φ in the first term using the fact that $\dot{U} + A(U)U' = 0$, and summing over n, we then obtain

$$0 = \int_{\mathbb{R}}\int_0^{t_N} -(U\dot{\varphi} + f(U)\varphi')dx\,dt$$

$$+\sum_{n=1}^{N}(\hat{\epsilon}U', (\pi_h\varphi)')_n^+ k_n + \sum_{n=1}^{N}([U_{n-1}], (\pi_h\varphi)_{n-1} - \varphi_{n-1}).$$

By the basic energy estimate (42), it follows as above using that φ is smooth (with compact support), that the second term on the right hand side tends to zero. Further, for the third term, we have by a standard interpolation estimate bringing in a factor h_n^2, recalling that $\alpha = \max_n \bar{h}_n^2/k_n$, and letting $\bar{k} = \max_n k_n$,

$$\sum_n |([U_{n-1}], (\pi_h\varphi)_{n-1} - \varphi_{n-1})| \leq C_i C_\varphi (\sum_n |[U_{n-1}]|^2)^{1/2}\alpha(\bar{k}\sum_n k_n)^{1/2},$$

where C_i is an interpolation constant and C_φ a constant depending on φ, which using (42) surely tends to zero as $\bar{h}$ and $\bar{k}$ tend to 0. This proves that a limit of chG(1,0) solutions is a weak solution of (8).

A limit of chG(1,0)-solutions satisfies all entropy inequalities To prove entropy consistency, let now $\eta(u)$ be a smooth strictly convex entropy with corresponding entropy flux $q(u)$. In (38) we then choose $v = \pi_h(\eta'(U)\varphi) \in W^\beta_{kn}$, where φ now is a non-negative smooth function with compact support, and obtain integrating by parts using again the fact that in the integration over the slab S_n the interpolation operator π_h can be removed, while changing from $\pi_h(\eta'(U)\varphi)$ to $\eta'(U)\varphi$ in the jump term on the discrete time levels brings in the factor $\psi_{n-1} = \eta'(U^+_{n-1})\varphi_{n-1} - \pi_n(\eta'(U^+_{n-1})\varphi_{n-1})$, with π_n the usual nodal interpolation operator into V_n,

$$\begin{aligned}
0 = &-\textstyle\int_0^{t_N}\int_{\mathbb{R}}\eta(U)\dot{\varphi}\,dx\,dt - \int_0^{t_N}\int_{\mathbb{R}} q(U)\varphi'\,dx\,dt \\
&+ \textstyle\sum_{n=1}^N(\hat{\epsilon}U', (\pi_n\eta'(U)\varphi)')_n^+ k_n - \sum_{n=1}^N([U_{n-1}], \psi^+_{n-1}) \\
&+ \textstyle\sum_{n=1}^N(\eta(U^-_{n-1}) - \eta(U^+_{n-1}) - \eta'(U^+_{n-1})(U^-_{n-1} - U^+_{n-1}), \varphi_{n-1}) \\
&= -I - II + III - IV + V,
\end{aligned}$$

with the obvious notation. Here, the terms I and II will generate the desired terms in the entropy inequality. By the convexity of η, and the positivity of φ, the term V is non-negative. We will now show, using in a crucial way the design of the artificial viscosity $\hat{\epsilon}$, that III will generate a positive term through which we will be able to dominate IV. We then first split III into

$$\begin{aligned}
\textstyle\sum_n(\hat{\epsilon}U', (\pi_n\eta'(U)\varphi)')_n^+ k_n &= \textstyle\sum_n(\hat{\epsilon}U', (\pi_n\eta'(U))'\varphi)_n^+ k_n \\
&+ \textstyle\sum_n(\hat{\epsilon}U', (\pi_n\eta'(U)\varphi)' - (\pi_n\eta'(U))'\varphi)_n^+ k_n = III_1 + III_2.
\end{aligned}$$

Now, it is straight forward to show that III_2 will vanish in the limit, using the fact that $(\pi_n\eta'(U)\varphi)' = (\pi_n\eta'(U))'\varphi$ if φ is constant, from which follows that in III_2 we may replace φ by $\varphi-\bar{\varphi}$ with $\bar{\varphi}$ a piecewise constant approximation. Thus, we may focus our interest on III_1, and we then make the crucial observation that

$$(\hat{\epsilon}U', (\pi_n\eta'(U))'\varphi)_n^+ k_n \geq c(\hat{\epsilon}U', U'\varphi)_n^+ k_n$$

where c is a lower bound of η'', recalling the strict convexity of η. This follows because on an interval $I_j = (x_{j-1}, x_j)$ underlying V_n of length h_{nj} with $W = U_{n-1}^+$ as above,

$$\begin{aligned} W'(\pi_n\eta'(W))' &= h_{nj}^{-2}(W(x_j) - W(x_{j-1}))(\eta'(W(x_j)) - \eta'(W(x_{j-1}))) \\ &\geq ch_{nj}^{-2}(W(x_j) - W(x_{j-1}))^2 = c(W')^2. \end{aligned}$$

We conclude the following crucial positivity property of the artificial viscosity term III:

$$III_1 \geq c\sum_n (\hat{\epsilon}U', U'\varphi)_{n-1}^+ k_n.$$

We now return to the critical term IV with the objective of bounding this term using the positive term III_1. To this end, we note that by a standard interpolation estimate, we have

$$\begin{aligned} &|([U_{n-1}], \psi_{n-1})| \leq C_i \int_{\mathbb{R}} h_n^2 \tfrac{|[U_{n-1}]|}{k_n}(|\eta'''(W)|(W')^2\varphi_{n-1} \\ &+C_\varphi|\eta''(W)W'| + C_\varphi|\eta'(W)|)k_n\,dx, \end{aligned} \tag{43}$$

which follows by computing the derivative $(\eta'(W)\varphi_{n-1})''$ element by element, noting in particular that $W'' = 0$ on each element. Now, if $\bar{h}$ is sufficiently small, then by the design property (36), using the strict convexity of η to see that $|\eta'''|/\eta''$ is bounded from above,

$$\int_{\mathbb{R}} h_n^2 \frac{|[U_{n-1}]|}{k_n} C_i|\eta'''(W)|(W')^2\varphi_{n-1}k_n \leq c(\hat{\epsilon}U', U'\varphi)_n^+ k_n. \tag{44}$$

The remaining terms on the left hand side of (43) may be dominated similarly (with a good margin) using also (42). Thus, the crucial term V can be dominated by the positive artificial viscosity term III_1 together with (42), and we conclude that a limit of chG(1,0)-solutions, satisfies

$$-\int_0^t \int_{\mathbb{R}} \eta(w)\dot{\varphi}\,dx\,dt - \int_0^t \int_{\mathbb{R}} q(w)\varphi'\,dx\,dt \leq 0,$$

which is the weak form of the entropy inequality for given entropy $\eta(u)$.

What is the minimal amount of artificial viscosity? The above analysis shows that the design property $\hat{\epsilon} \geq Ch^{2-\kappa}R$ with κ small positive, is sufficient to guarantee entropy consistency for chG(1,0), the critical inequality being (44) containing the ingredients h_n^2, $R(U) = |[U_{n-1}]|/k_n$, $\hat{\epsilon}$, and $((U_{n-1}^+)')^2$. The analysis also indicates that to guarantee entropy consistency, we need $h^2 R/\hat{\epsilon}$ to be sufficiently small.

The design of the artificial viscosity for the Sd-method with non-oriented space-time mesh is similar: $\hat{\epsilon} \sim h^2 R(U)$, with $R(U)$ the full residual including also a contribution $|\dot{U} + (f(U))'|$ from the space-time slab.

The essence of the argument showing entropy consistency can be exhibited in the setting of a Galerkin method for a nonlinear problem $L(u) = 0$, for which the entropy inequality for a given entropy $\eta(u)$ is obtained multiplying by $\eta'(u)\varphi$, where φ is a smooth non-negative test function with compact support. To prove entropy consistency we choose $v = \pi_h(\eta'(U)\varphi) \in V_h$ in the Galerkin equations $(L(U), v) + (\hat{\epsilon}U', v') = 0$ for all $v \in V_h$, where V_h is the finite element space underlying the Galerkin method, π_h is an interpolation opertator into V_h, and $\hat{\epsilon}$ is the artificial viscosity. Replacing then $\pi_h(\eta'(U)\varphi)$ by $\eta'(U)\varphi$ in the first term, brings in the crucial compensating term

$$E = (L(U), \eta'(U)\varphi - \pi_h(\eta'(U)\varphi)),$$

which will have to be dominated by the positive term $(\hat{\epsilon}U', \eta'' U'\varphi)$ resulting from the artificial viscosity term. By standard interpolation estimates computing the derivative $(\eta'(U)\varphi)'$, we have, writing out only the most critical term with no differentiation of φ,

$$E \leq (C_i h^2 R(U) U', U'\varphi)$$

where $R(U) = |L(U)|$ is the residual. If now $\hat{\epsilon} = Ch^2 R(U)$ with C large enough, then this term will be dominated by the indicated positive term, and the desired entropy inequality will follow.

3.5 Adaptive algorithms

Adaptive algorithms for chG(1,0) are based on a posteriori error estimates of the form

$$\|u - U\| \leq C_i S_c \|\frac{h^2}{\hat{\epsilon}} R(U)\| + E(\hat{\epsilon} - \epsilon), \tag{45}$$

where $E(\hat{\epsilon} - \epsilon)$ accounts for the perturbation effect of the artificial viscosity with $E(0) = 0$, and S_c is a strong stability factor. The norm $\|\cdot\|$ may be an $L_q(L_p)$-norm in time-space. Similar estimates may be derived for the Sd and orG-methods. The modification criterion of the adaptive algorithm may include modification of (i) mesh size and (ii) $\hat{\epsilon}$. In particular, we may seek to adaptively achieve $\hat{\epsilon} = \epsilon$, in which case the second term in (45) disappears. This may be attempted if ϵ is not too small, and corresponds to pointwise resolution of the exact solution. The mesh modification may be based on equidistribution, seeking to make the element contribution to the norm $\|h^2 \hat{\epsilon}^{-1} R(U)\|$ equal. In orG variants also the mesh orientation may be modified for example according to the space-time gradients of computed solutions. For numerical results illustrating the effect of different orientations in space-time, see [22].

3.6 A posteriori error estimates

As an illustration of the general approach, we now prove an a posteriori error estimate for the following variant of the chG(1,0) method for (6) with $\epsilon > 0$ and $A(U) = U$ considering Burgers' equation: find $U = U(x,t)$ such that, for $n = 1, 2, \ldots$, $U|_{S_n}$ satisfies

$$\begin{aligned} \dot{U} + UU' - \epsilon U'' &= 0, (x,t) \in \mathbb{R} \times I_n, \\ U(x,t) \to 0, &x \to \pm\infty,\ t \in I_n, \\ U_{n-1}^+ &= P_n U_{n-1}^-, \end{aligned} \tag{46}$$

where $U_0^- = u_0$. In this method we L_2-project at each discrete time level t_{n-1} into a space V_n of continuous piecewise linears of mesh size $h_n(x)$, and solve the conservation law exactly on each slab S_n, which corresponds to a method of the form projection-transport. For simplicity we will assume that $\hat{\epsilon} = \epsilon$, a condition which may be included in the stopping criterion if ϵ is not too small, as indicated above. We use the notation $Q = \mathbb{R} \times (0,T)$ and write $\|v\|_Q = \|v\|_{L_2(Q)}$.

Let now $T = t_N > 0$ be a given final time, and let us seek an *a posteriori* error estimate for the error $\|u - U\|_Q$. To this end, we start representing the error in terms of the solution φ of the following linearized dual problem:

$$\begin{aligned} -\dot{\varphi} - a\varphi' - \epsilon\varphi'' = e,\ x \in R,\ 0 < t < T, \\ \varphi(x,t) \to 0,\ x \to \pm\infty,\ 0 < t < T, \\ \varphi(x,T) = 0,\ x \in \mathbb{R}, \end{aligned} \tag{47}$$

where $a = (u+U)/2$. Multiplying (47) by e, we obtain by integration by parts over each S_n, $n = 1, \ldots, N$, since $(ae)' = \frac{1}{2}(u^2 - U^2)' = uu' - UU'$,

$$\|e\|_Q^2 = \textstyle\sum_{n=1}^N \int_{S_n} e\left(-\dot{\varphi} - a\varphi' - \epsilon\varphi''\right)\ \mathrm{d}x\mathrm{d}t$$

$$\sum_{n=1}^N \int_{S_n} \Big((\dot{u} + uu' - \epsilon u'') - (\dot{U} + UU' - \epsilon U'')\Big)\,\varphi\ \mathrm{d}x\mathrm{d}t$$

$$+ - \sum_{n=1}^N \int_{\mathbb{R}} (I - P_n)U_{n-1}^- \varphi_{n-1} \mathrm{d}x,$$

where we used that $U_{n-1}^+ = P_n U_{n-1}^-$. Thus, by (6), (46) and the orthogonality of the L_2 projection P_n, we obtain the following representation of the error:

$$\|e\|_Q^2 = -\sum_{n=1}^N \int_{\mathbb{R}} (I - P_n)U_{n-1}^- (I - P_n)\varphi_{n-1}\ \mathrm{d}x.$$

Recalling now the basic estimate for the L_2 projection error $(I-P_n)\varphi_{n-1}$:

$$\|(I-P_n)\varphi_{n-1}\| \le C_i\|h_n^2\varphi_{n-1}''\|,$$

we obtain by Cauchy's inequality

$$\|e\|_Q^2 \le C_i\left(\sum_{n=1}^N \|\frac{h_n^2}{\epsilon k_n}(I-P_n)U_{n-1}^-\|^2 k_n\right)^{1/2}\left(\sum_{n=1}^N \left\|\epsilon\varphi_{n-1}''\right\|^2 k_n\right)^{1/2}.$$

Defining the strong stability factor S_c by

$$S_c = \frac{\left(\sum_{n=1}^N \left\|\epsilon\varphi_{n-1}''\right\|^2 k_n\right)^{1/2}}{\|e\|_Q}, \tag{48}$$

and writing

$$\|\frac{h^2}{\epsilon k}(I-P)U\|_{L_2(Q)} = \left(\sum_{n=1}^N \|\frac{h_n^2}{\epsilon k_n}(I-P_n)U_{n-1}^-\|^2 k_n\right)^{\frac{1}{2}},$$

we then obtain the following a posteriori error estimate:

Theorem 1. *The solution U of (46) satisfies*

$$\|u-U\|_Q \le S_c C_i\|\frac{h^2}{\epsilon k}(I-P)U\|_Q, \tag{49}$$

where S_c is defined by (48).

This gives an estimate of the computational error $u-U$ in terms of the projection or interpolation error $(I-P)U$, modulo the strong stability constant S_c, and the factor $\frac{h^2}{\epsilon k}$. Below we show that S_c is bounded by a moderate constant in the basic cases of a (i) smooth exact solution, (ii) shock, and (iii) rarefaction, where in the last case the $L_2(Q)$-norm is modified to a weighted variant. Assuming that the factor $\frac{h^2}{\epsilon k}$ is less than one, which may be natural, (49) simplifies to

$$\|u-U\|_Q \le S_c C_i\|(I-P)U\|_Q. \tag{50}$$

3.7 A priori error estimate

The above a posteriori error estimate can be turned into an a priori error estimate if we can a priori demonstrate some regularity of U_{n-1}^-, from which we may deduce an estimate for $\|(I-P)U_{n-1}^-\|$, and thus for $\|(I-P)U\|$. The basic energy estimate guarantees that the quantity

$$\sum_n(\hat{\epsilon}\nabla U_{n-1}^+, \nabla U_{n-1}^+)$$

is bounded. A similar bound holds with U_{n-1}^+ replaced by U_n^-, if $k_n\|U\|_\infty \le h$ guaranteeing that the mesh distortion over one slab S_n is controled.

3.8 Stability estimates for smooth solutions, shocks and rarefactions

We now investigate the stability properties of the linearized dual Burgers' equation in some basic cases including smooth solutions, shocks and rarefactions. Recalling (47), the dual problem takes the following form if we now linearize at an exact solution $u(x,t)$ (instead of the mean value $(u+U)/2$):

$$\begin{aligned} -\dot\varphi - u\varphi' - \epsilon\varphi'' &= e,\ \ x\in\mathbb{R},\ \ 0<t<T, \\ \varphi(x,T) &= 0,\ \ x\in\mathbb{R}. \end{aligned} \tag{51}$$

The stability properties are largely determined by the sign of u', which reflects the change of the direction u of the characteristics. If $u'\leq 0$, then the characteristics converge with increasing t, which typically occurs in the case of a shock. If $u'\geq 0$, then the characteristics diverge, which typically occurs in the case of a rarefaction. If u' is bounded below by a moderate constant, e.g. $u'\geq 0$, then we may estimate $\|\varphi\|_{L_\infty(L_2(\mathbb{R}))}$ and $\|\sqrt{\epsilon}\varphi'\|_Q$ in terms of a moderate constant times $\|e\|_Q$, which we refer to as *weak stability*. If u' is bounded above by a moderate constant, e.g. $u'\leq 0$, then we may estimate $\|\epsilon\varphi''\|_Q$ in terms of a moderate constant times $\|e\|_Q$, which we refer to as *strong stability*, because we estimate second derivatives of φ, cf. (48). These estimates are proved by multiplying by φ and $-\epsilon\varphi''$, respectively, bringing in the positive stabilizing terms $\frac{1}{2}u'\varphi^2$ and $-\frac{1}{2}\epsilon u'(\varphi')^2$, respectively.

Shocks We now prove a strong stability estimate showing that the continuous analog $\|\epsilon\varphi''\|_Q/\|e\|_Q$ of the stability factor S_c defined by (48), is of moderate size if u' is bounded above. This assumption is satisfied if u is piecewise smooth with shocks, recalling that u is decreasing in a shock, so that there u' is large negative and in particular $u'\leq 0$. We plot the characteristics of the dual problem in this case below. We thus give evidence that the stability factor S_c of the a posteriori error estimate (49) is of moderate size if u is piecewise smooth with shocks, which indicates that such a solution is computable with a computational cost comparable to that of direct interpolation. Thus, a piecewise smooth solution with shocks is not so costly to compute.

Lemma 2. *Let $A=\max_Q u'$. The solution φ of (51) satisfies*

$$\|\epsilon\varphi''\|_Q + \|\dot\varphi + u\varphi'\|_Q + \sup_{0<t<T}\|\epsilon^{1/2}\varphi'(\cdot,t)\|_R \leq 3\exp(AT)\|e\|_Q. \tag{52}$$

Proof. Multiplying the first equation in (51) by $-\epsilon\varphi''$, integrating by parts with respect to x, and integrating in time over (τ,T), we get with $Q_\tau = R\times(\tau,T)$

$$\begin{aligned} &\tfrac{1}{2}\int_R \epsilon\left(\varphi'(\cdot,\tau)\right)^2 dx + \int_{Q_\tau}\left(\epsilon\varphi''\right)^2\, dxdt + \int_{Q_\tau}\tfrac{1}{2}\left(u\epsilon\left(\varphi'\right)^2\right)'\ dxdt \\ &\leq \tfrac{1}{2}\int_{Q_\tau}\left(\epsilon u'\left(\varphi'\right)^2 + e^2 + \left(\hat\epsilon\varphi''\right)^2\right)\ dxdt, \end{aligned} \tag{53}$$

which proves the lemma using a Grönvall's inequality, since the last term on the left hand side integrates to zero.

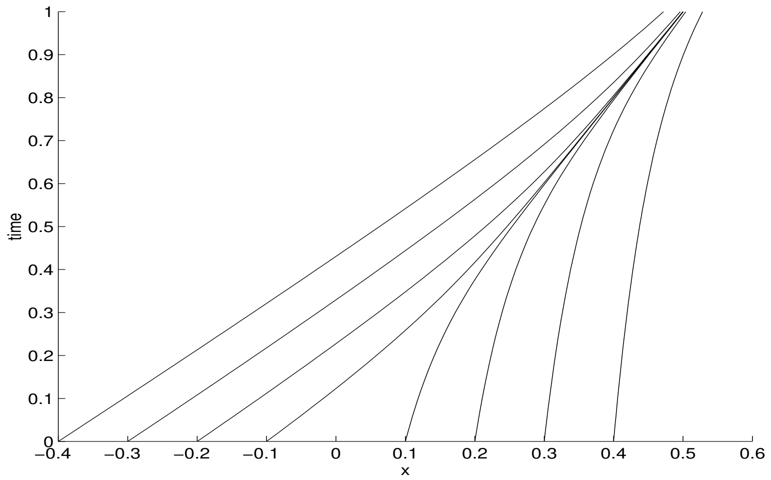

Let us now attempt to derive a weak stability estimate for (51) in the case u is a shock. Multiplication by φ and integration over Q_τ gives

$$\begin{aligned}&\tfrac{1}{2}\int_R \varphi^2(x,\tau)\ dx + \epsilon\int_{Q_\tau}\left(\varphi'(x,t)\right)^2\ dxdt\\ &= -\tfrac{1}{2}\int_{Q_\tau} u'\varphi^2(x,t)\ dx + \int_R e(x,t)\varphi(x,t)\ dx.\end{aligned}$$

Since u' is large negative in the case of a shock, we have large positive term of the right hand side, and using Grönwall's lemma, results in a very large stability factor (of size $\exp(-u')$). The situation is more favorable concerning weak stability estimates for a rarefaction wave solution with $u' \geq 0$, as we demonstrate below.

Summing up, we see that for a shock, the linearized dual problem statisfies a strong stability estimate with a stability factor of moderat size, while a corresponding weak stability estimate appears to have a very large stability factor. These stability features may be understood in a qualitative sense, by pondering the directionality of the characteristics and the nature of the L_2-norm.

Rarefaction wave We now consider the linearized dual Burgers' equation (51), linearized at the exact solution $u(x,t) = x/t$, corresponding to a rarefaction wave. Multiplying now (51) by $-\epsilon t\varphi''$, and using standard manipulations, we obtain the following weighted norm strong stability estimate for

$0 < \tau < T$,

$$\|\tau^{1/2}\epsilon^{1/2}\varphi'\| + \|\omega\epsilon\varphi''\|_{Q_\tau} \leq \|\omega e\|_{Q_\tau}, \tag{54}$$

where $\omega(t) = t^{1/2}$ acts as a weight, and $Q_\tau = \mathbb{R} \times (\tau, T)$.

A weighted norm analog of the a posteriori error estimate (50 takes the form

$$\|\omega^{-1}e\|_{L_2(Q_\tau)} \leq S_c\|\omega^{-1}(I-P)U\|_{L_2(Q_\tau)} \tag{55}$$

with S_c defined by the direct weighted norm analog of (48). The estimate (54) then shows that S_c is of moderate size, and thus a rarefaction wave solution is computable in the weighted norm with computational work corresponding to interpolation. Note that the presence of the weight $t^{-1/2}$ will force more stringent demands on the mesh for t close to zero, which will force an accurate resolution of the initial phase of the rarefaction. This is intuitively reasonable and corresponds to the fact that an initial error in the computation of a rarefaction will get amplified as time goes, because characteristics diverge forward in time. On the other hand, in the case of a shock, an initial error may be eliminated at later times, because of converging characteristics, Thus, a rarefaction is more delicate to compute than a shock.

3.9 Dual-weighted a posteriori error estimates

One may also derive a posteriori error error estimates with derivatives of the dual solution occuring as weights in the error representation integral. Starting from (56), such a dual-weighted a posteriori error estimate takes the form

$$\|e\|_Q^2 \leq C_i \sum_{n=1}^{N} \int_{\mathbb{R}} \frac{h_n^2}{\epsilon k_n} |(I-P_n)U_{n-1}^-|\omega_{n-1}\ \mathrm{d}x\, k_n. \tag{56}$$

where $\omega_{n-1} = \epsilon|\varphi''_{n-1}|$, and φ is the solution of the dual problem (47). This estimate may give a more precise error representation, and thus lead to a more optimally adapted mesh size $h(x)$, than the estimate (49) with the stability factor S_c as a scalar factor outside the norm.

3.10 A posteriori error estimates in a negative norm

In principle, we may seek to control the error in any given norm by computing the corresponding sability factor by solving a dual problem with suitable data. The norm $L_\infty(H^{-1}(\mathbb{R}))$ offers certain advantages from analysis point of view, and connects to the following data for a dual linearized Burgers' equation, linearized at the solution $u(x,t)$:

$$\begin{aligned} -\dot\varphi - u\varphi' - \epsilon\varphi'' &= 0,\ x \in R,\ 0 < t < T, \\ \varphi(x,t) &\to 0,\ x \to \pm\infty,\ 0 < t < T, \\ \varphi(x,T) &= E,\ x \in R, \end{aligned} \tag{57}$$

where $-E'' = e(T)$, $E(x,t) \to 0$ as $x \to \pm\infty,\ 0 < t < T$. In this problem, we may multiply by φ'', and derive in the shock wave case with $u' \leq 0$, a stability estimate of the form

$$\max_{0<\tau<T}(\|\varphi'(\tau)\|^2 + \|\sqrt{\epsilon}\varphi''\|^2_{Q_\tau}) \leq \|\varphi'(T)\|^2 = \|e\|^2_{H^{-1}}. \tag{58}$$

An analog of the a posteriori error estimate (49) in the norm $L_\infty(H^{-1}(\mathbb{R}))$, reads

$$\|(u-U)(T)\|_{H^{-1}(\mathbb{R})} \leq S_c C_i \|\frac{h^2}{\sqrt{\epsilon}k}(I-P)U\|_{L_\infty(L_2(\mathbb{R}))}, \tag{59}$$

with the stability factor is defined by

$$S_c = \frac{\int_0^T \|\sqrt{\epsilon}\varphi''\|dt}{\|\varphi'(T)\|}. \tag{60}$$

We notice a gain of a factor $\sqrt{\epsilon}$ as compared to (49) due to the asymmetry of norms in (59), with the weaker $H^{-1}(\mathbb{R})$-norm on the left hand side.

We now present computed approximations of S_c defined by (60) for a typical solution of Burgers' equation, together with plots of dual solutions. Below we present similar results for the compressible Euler equations in 1d, and further results in 2d including two-phase flow are presented in [3]. In all these cases, S_c turns out to be of moderate size, indicating computability of the corresponding solutions (none of which is turbulent). The stability factor S_c related to the norm $L_2(L_2(\mathbb{R}))$ defined by (48), is of a similar size in these examples.

3.11 Dual solution and stability factors for Burgers' equation

We consider a case with the exact solution consisting of a rarefaction wave and a shock and $10^{-4} \leq \epsilon \leq 10^{-5}$. We use the cG(1)dG(0) Sd-method on a uniform space mesh with $h = 10^{-3}$ and time step 10^{-4}. We plot the computed solution at t=0, t=0.3 , t=0.8, t=1.

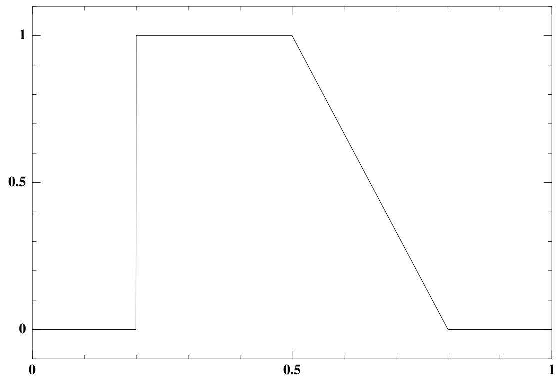

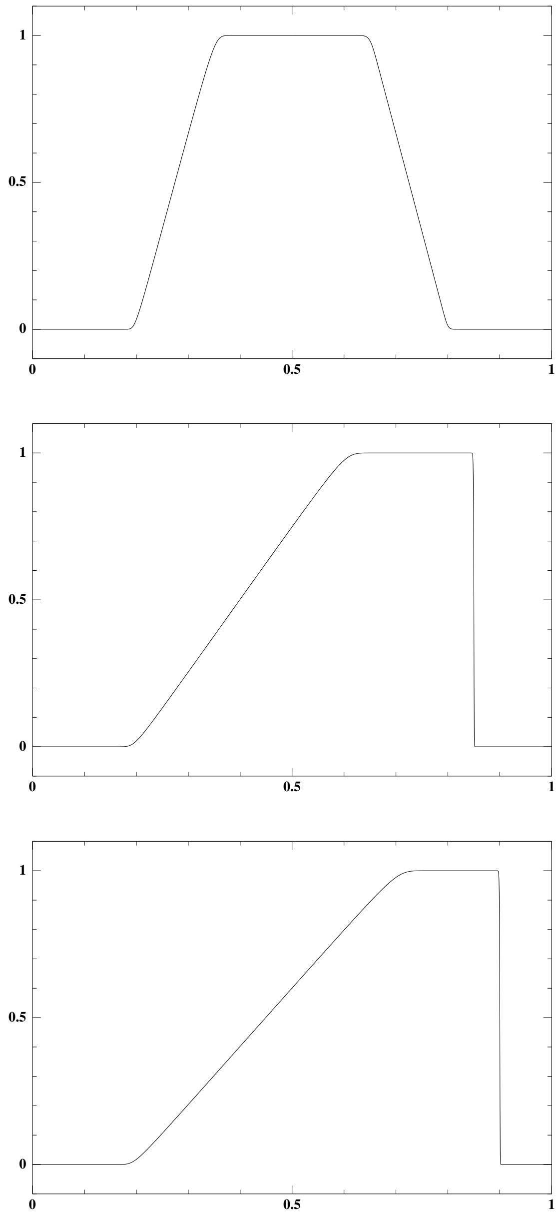

We have solved the dual problem using the following approximations of the coefficient $a = (u + U)/2$ and the error e, with $\bar{u}$ the analytical, inviscid solution, and $U(h)$ the finite element solution on a mesh of size h: (i) $a = (\bar{u} + U(h))$ and $e = \bar{u} - U(h)$, (ii) $a = U(h)$ and $e = \bar{u} - U(h)$, (iii) $a = (U(h/4) + U(h))/2$ and $e = U(h/4) - U(h)$. We plot the corresponding dual solution φ at the same time levels as above, but in reverse order (t=1, t=0.8 , t=0.3 , t=0):

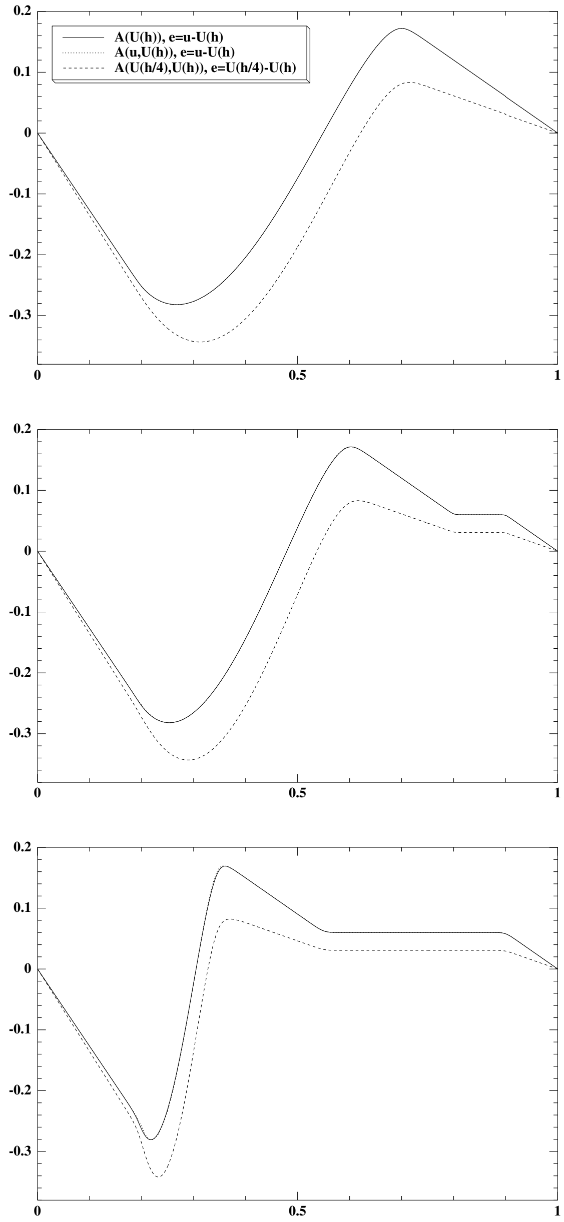

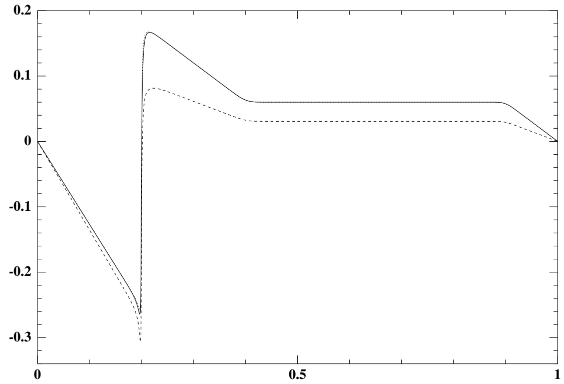

In the following figure we plot the corresponding second derivatives φ'' including a zoom at $t = 0$ around $x = 0.2$:

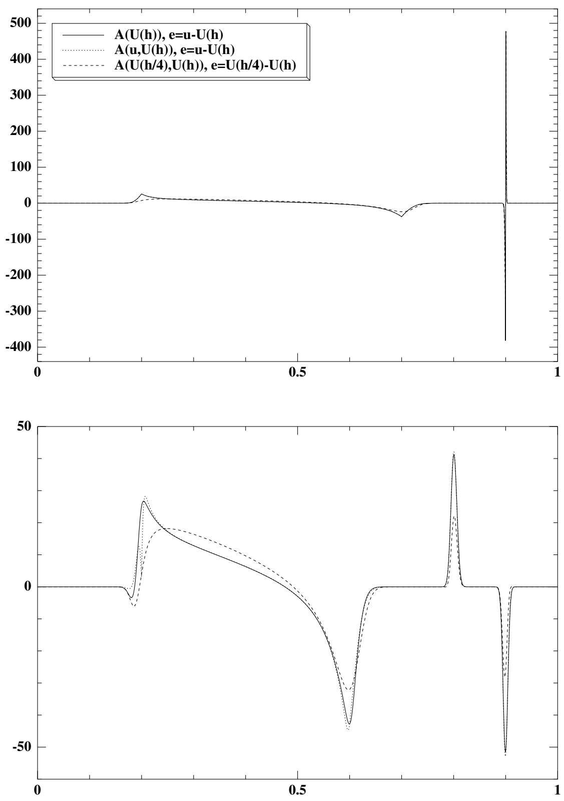

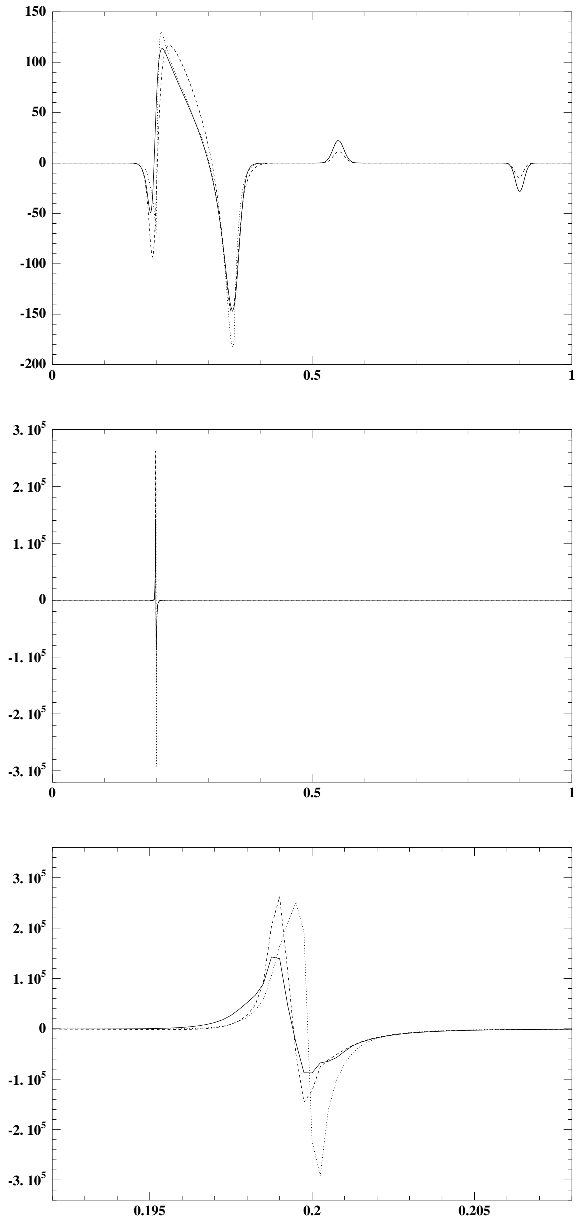

We note the change of the weight $|\varphi''|$ from being large close to the shock at final time towards being large close to the initial discontinuity at $(x, t) = (0.2, 0)$. Note that that it is the data from the rarefaction at final time which generates the large values of φ'' at $t = 0$, and not those from the shock.

We next plot the stability factor S_c defined by (60) for the three different approaches using three different values on the viscosity ($\epsilon = 0.0001$, $\epsilon = 0.00005$, $\epsilon = 0.00001$):

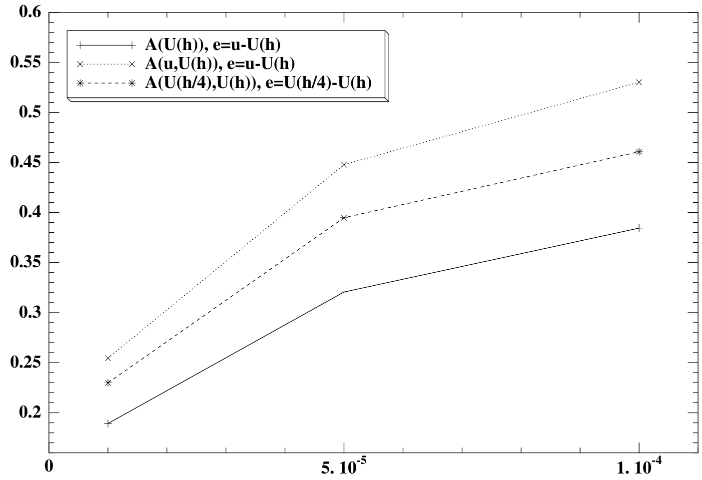

The stability factor defined by (48) is of similar size. The results indicate that the Burgers' solution is computable in $L_\infty(H^{-1}(\mathbb{R}))$ and $L_2(L_2(\mathbb{R}))$ with work comparable to interpolation.

3.12 Scalar conservation laws in several dimensions

The material presented above directly generalizes to scalar conservation laws in $\mathbb{R}^d$, $d \geq 1$, of the form

$$\begin{aligned} \dot{u} + \textstyle\sum_{i=1}^d f_i(u)_{,i} - \epsilon \Delta u = 0, \quad x \in \mathbb{R}^d,\ t > 0, \\ u(x,0) = u_0(x), \quad x \in \mathbb{R}, \end{aligned} \tag{61}$$

where $f_i(u)$ is the flux in the x_i direction, and $v_{,i} = \frac{\partial v}{\partial x_i}$. Again, any convex function $\eta(u)$ may be chosen as an entropy, and the corresponding entropy inequality takes the strong form

$$\frac{\partial}{\partial t}\eta(u) + \sum_i \frac{\partial}{\partial x_i} q_i(u) \leq 0, \tag{62}$$

where the $q_i(u)$ are the entropy fluxes satisfying $q_i' = f_i' \eta'$.

3.13 The dG-method for scalar conservation laws

We now further generalize to a Galerkin method based on discontinuous piecewise polynomial approximation of degree q in both space and time, for the inviscid scalar conservation law (61) with $\epsilon = 0$. We refer to this method as the dG(q)-method. The dG(0) method coincides with the basic *finite volume method* based on piecewise constant approximation, which attracted much attention in the early development of numerical methods for conservation laws. The dG(q) with $q > 0$ generalizes the basic finite volume method, and gives a solution to the problem of designing high order finite volume methods including the problem of defining fluxes at discontinuities (so called numerical fluxes) and the design of the artificial viscosities, which has been the subject of extensive work in the literature on numerical methods for conservation laws. For a more detailed presentation of the dG method for scalar conservation laws, we refer to [33].

To discretize (61) with the dG-method, let as usual $0 = t_0 < t_1 < \ldots < t_n < \ldots$, be a sequence of discrete time levels, let $\mathcal{T}_n = \{K\}$ be a (space-time) finite element triangulation of the slab $S_n = \mathbb{R}^2 \times I_n$, where $I_n = (t_{n-1}, t_n)$, into finite elements K of diameter h_K. Typically, the elements K may be tetrahedra or prisms $\kappa \times I_n$, where κ is a triangle, or space-time oriented prisms. Define for a given $q \geq 0$,

$$W_n = \{v \in L_2(S_n) : v|_K \in P_q(K), \quad \forall K \in T_n\},$$

where $P_q(K)$ is a space of polynomials of degree at most q associated with $K \in \mathcal{T}_n$, and write $W = \prod_{n \geq 0} W_n$. As above we assume that the functions $v(x,t)$ in W_n vanish for $|x|$ large. With piecewise constant approximation corresponding to $q = 0$, we obtain the dG(0)-method. Choosing piecewise linear approximation on tetrahedra or piecewise bilinear approximation on prisms, we obtain different versions of dG(1). We may also obtain hybrid variants on prisms with piecewise linear approximation in space and piecewise constant approximation in time, and oriented versions thereof.

To formulate the dG(q) method we first rewrite (61) in the compact form div $f(u) = 0$, where (assuming for definiteness that $d = 2$), $f(u) = (f_i(u)) \equiv (f_0(u), f_1(u), f_2(u))$ with $f_0(u) = u$ and div now denotes the divergence with respect to $x \equiv (x_0, x_1, x_2)$ with $x_0 = t$, i.e.,

$$\text{div } f(u) = \sum_{i=0}^{2} f_i(u)_{,i} = u_t + \sum_{i=1}^{2} f_i(u)_{,i}. \tag{63}$$

The dG(q)-method for (61) can now be formulated as follows: find $U \in W$ such that for $n = 0, 1, \ldots$,

$$\begin{aligned} \sum_{K \in T_n} \{ \int_K \text{div} f(U)(v + \delta \sum_{i=0}^{2} f_i'(U) v_{x_i}) dx + \int_K \hat{\epsilon} \nabla U \cdot \nabla v dx \qquad (64) \\ + \int_{\partial K} (F_K(U) - f(U_K) \cdot n_k) v_k ds \} = 0, \qquad \forall v \in W_n, \end{aligned}$$

where ∇ is the gradient w.r.t. $x = (x_0, x_1, x_2)$, $U_K = U|_K$, $n_K = n_K(x)$ is the outward unit normal to K at $x \in \partial K$, $F_K(U)$ is the numerical flux (referred to as the Lax-Friedrichs' flux) given by

$$F_K(U)(x) = \frac{1}{2}(f(U_K(x)) + f(U_{K'}(x))) \cdot n_K(x) + C_K(x)(U_K - u_{K'})(x), \quad (65)$$

for $x \in \partial K \cap \partial K'$, where K' (for a given $x \in \partial K$) denotes the neighboring element to K, ($K' \in \mathcal{T}_m$ with $m = n-1, n$ or $n+1$), and for $x \in \partial K \cap \partial K'$, $f \cdot n_K = \sum_{i=0}^{2} f_i n_{K,i}$, $n_K = (n_{K,i})$,

$$\begin{array}{rl} C_K(x) = \frac{1}{2} & \text{if } n_K(x) = \pm(1,0,0), \\ C_k(x) = C_{K'}(x) = C_0 & \text{otherwise,} \end{array}$$

where C_0 is a positive constant satisfying

$$\begin{array}{rl} C_0 > \frac{1}{2}\|f'\|_\infty = \max_{r\in\mathbb{R}} |f'(r)|, & |f'| = (\sum_{i=0}^{2}(f_i')^2)^{\frac{1}{2}}, \\ U_K = U|_K,\, U_K(x) = \lim_{\substack{y\to x \\ y\in K}} U(y),\, U_{K'}(x) = \lim_{\substack{y\to x \\ y\in K'}} U(y), & \\ U_{K'}(\bar{x},0) = u^0, & \\ \delta(U) = \frac{1}{2}(k_n^{-2} + h_n^{-2}|f'|)^{-1/2}, & \\ \hat{\epsilon}(U) = \max(\gamma_1 h^2 R(U), \gamma_2 h^{3/2}), & \\ R(U)|_K = \max_K |\text{div } f(U)| + \max_{\partial K} |f(U_K) - f(U_{K'})/h_K. & \end{array}$$

The dG(0) method is an implicit variant of the classical finite volume method based on piecewise constant approximation and the Lax-Friedrichs' flux, and the dG(q) method is a generalization of order of accurcy at least $q + \frac{1}{2}$.

4 The Euler equations for an inviscid perfect gas

In this section we extend the material presented above to the Euler equations for an inviscid perfect gas, including details on the formulation of the G^2-method, and computational results on dual solutions and stability factors. The results on entropy consistency and a posteriori error estimation generalize in a direct way. We also discuss the use of entropy variables.

The Euler equations for a compressible inviscid perfect gas in $\mathbb{R}^3$ read on conservation form: find $u(x,t)$ such that

$$\begin{array}{rl} \dot{u} + \sum_{i=1}^{3} f_i(u)_{,i} = 0 & x \in \mathbb{R}^3,\, t > 0, \\ u(x,0) = u_0(x) & x \in \mathbb{R}^3, \end{array} \quad (66)$$

where u_0 is given initial data,

$$u = \rho \begin{bmatrix} 1 \\ w_1 \\ w_2 \\ w_3 \\ e \end{bmatrix},\quad f_i = w_i u + p \begin{bmatrix} 0 \\ \delta_{1i} \\ \delta_{2i} \\ \delta_{3i} \\ w_i \end{bmatrix},$$

ρ is the density, $w = (w_1, w_2, w_3)$ is the particle velocity, e is the total energy density, $p = (\gamma - 1)(\rho e - \rho|w|^2)/2)$ is the pressure, δ_{ij} the Kronecker delta,

$\gamma > 1$ is a constant, and $v_{,i} = \partial v/\partial x_i$. These equations generalize the one-dimensional equations (13) and express conservation of mass, momentum and energy. For smooth solutions the conservation law (66) can be written as a generalized convection problem of the form

$$\dot{u} + \sum_{i=1}^{3} A_i(u)u_{,i} = 0, \tag{67}$$

where the $A_i = \frac{\partial f_i}{\partial u}$ are the Jacobians of the $f_i(u)$.

The function $\eta(u) = \rho \log(p\rho^{-\gamma})$ is a mathematical entropy for 66 corresponding to the negative of the physical entropy, which up to trivial modfications is the only known entropy for 66. The function $\eta(u)$ is a convex function of u, with symmetric positive definite Hessian η''. Smooth solutions of (66) or equivalently (67), satisfy the equation

$$\frac{\partial}{\partial t}\eta(u) + \sum_{i=1}^{3} \frac{\partial}{\partial x_i}(q_i(u)) = 0.$$

where $q(u) = (q_i(u)) = \eta w = (\eta w_i)$ is the entropy flux. This equation follows by multiplying 67 by the gradient $\eta'(u)$ of $\eta(u)$ and using the compatibility relation

$$\eta'(u)^* A_i(u) = q_i'(u)^*, \tag{68}$$

with $*$ denoting the transpose. The compatibility condition 68 is equivalent to the relation

$$\eta'' A_i = A_i^* \eta'', \quad i = 1, 2, 3, \tag{69}$$

stating that the Hessian η'' simultaneously symmetrizes all the A_i. The entropy inequality characterizing physical weak solutions reads in strong form

$$\frac{\partial}{\partial t}\eta(u) + \sum_{i} \frac{\partial}{\partial x_i}(q_i(u)) \leq 0. \tag{70}$$

4.1 The G^2-method

Let $\{S_n\}$ be a sequence of space-time slabs $S_n = \mathbb{R}^3 \times I_n$, where $I_n = (t_{n-1}, t_n)$, with associated space-time piecewise polynomials $V_n \subset [\mathcal{C}(S_n)]^5$, and let $V = \prod_{n \geq 1} V_n$. The G^2-method for (66) can be formulated as follows (extending the notation used above): find $U \in V$ such that for $n = 1, 2, ...,$

$$\begin{aligned} &(\dot{U} + \textstyle\sum_i A_i(U)U_{,i}, v + \delta(\dot{v} + \sum_i A_i^*(U)v_{,i}))_n \\ &+(\hat{\epsilon}\nabla U, \nabla v)_n + ([U_{n-1}], v_{n-1}^+) = 0 \quad \forall v \in V_n, \end{aligned} \tag{71}$$

where $*$ denotes transpose, and

$$\delta^* = \delta(U)^* = \frac{1}{2}(k_n^{-2} I + h_n^{-2} \sum_{i=1}^{2} A_i(U)^2)^{-\frac{1}{2}} \quad \text{on } S_n, \tag{72}$$

$$\hat{\epsilon} = \max(\gamma_1 h^2 |R(U)|, \gamma_2 h^{3/2}),$$
$$R(U) = |\dot{U} + \sum_i A_i(U) U_{x_i}| + |[U^n]|/k_n \quad \text{on} \quad S_n.$$

Depending on the space-time orientation of the finite-elements we get different versions of the G^2-method, including the Eulerian Sd-method, the chG-method orienting along particle paths, and various orG-methods with orientation according to solution features. The simplest instance of the method is the Sd(1,0) method obtained with a $\mathcal{P}_1 \times \mathcal{P}_0$- approximation in space-time with the basis functions continuous piecewise linear in x and discontinuous piecewise constant in time. Writing $U^n \equiv U|_{S_n}$, the G^2-method (71) can in this case be formulated as follows: Find $U^n \in W_n$ such that

$$\begin{array}{l}(U^n - U^{n-1}, v) + (\sum_i A_i(U^n) U^n_{,i}, v + \delta(\sum_i A_i(U^n)^* v_{,i}))k_n \\ +(\hat{\epsilon}\nabla U^n, \nabla v)k_n = 0 \quad \forall v \in W_n,\end{array} \tag{73}$$

where $W_n \subset [H^1(\mathbb{R}^3)]^5$ consists of continuous piecewise linears. To compute U^n from (73) approximately, we may iterate in various ways: the simplest possible variant is obtained by lumping the mass matrix related to the inner product $(\cdot,\cdot)$ in the first term on the left, and changing the index n to $n-1$ in the other terms, which gives a fully explicit version of Sd(1,0) of the form

$$\begin{array}{l}U^n_j = U^{n-1}_j - k_n(\sum_i f_i(U^{n-1})_{,i}, \varphi_j) \\ -k_n(\sum_i A_i(U^{n-1})U_{x_i}, \delta \sum_i A_i(U^{n-1})^* \varphi_{j,i}) - k_n(\hat{\epsilon}\nabla U^{n-1}, \nabla\varphi_j),\end{array} \tag{74}$$

where $U^n = \sum_j U^n_j \varphi_j(x)$ with $\{\varphi_j(x)\}$ the standard $\mathcal{P}_1$-basis functions of W_n.

To see that square root in (72) is well defined, we note that 69 implies that $A_0 = (\eta'')^{-1}$ symmetrizes the A_i, so that $\bar{A}_i \equiv A_i A_0$ is symmetric, $i = 1, 2, 3$. Therefore

$$A_0^{-\frac{1}{2}} A_i A_0^{\frac{1}{2}} = A_0^{-\frac{1}{2}} \bar{A}_i A_0^{-\frac{1}{2}}$$

is symmetric, and thus the similarity transform induced by $A_0^{\frac{1}{2}}$ transforms the matrix $M \equiv (k_n^{-2} I + h^{-2} \sum_i A_i^2)$ to an obviously positive definite symmetric matrix. It follows that M has positive eigenvalues and a full set of eigenvectors which shows that $M^{-\frac{1}{2}}$ can be computed. In [21] explicit formulas for the eigenvalues and eigenvectors of M are given.

4.2 Entropy variables

The change of variables $\bar{u} = \eta'(u)$, which is one-to-one since η'' is positive definite, transforms 67 into

$$\bar{A}_0 \dot{\bar{u}} + \sum \bar{A}_i \bar{u}_{,i} = 0 \tag{75}$$

where $\bar{A}_0(\bar{u}) = (\eta'')^{-1}(\bar{u})$ is positive definite symmetric, and $\bar{A}_i = A_i \bar{A}_0$ are symmetric because of (69). We refer to $\bar{u} = \eta'(u)$ as the *entropy varibles.*

In the entropy variables $\bar{u} = \eta'(u)$, the conservation law (67) takes the form of the symmetric hyperbolic system (75) with the $\bar{A}_i$ symmetric and $\bar{A}_0$ positive definite. The entropy inequality is obtained multiplying a viscous variant of (75) by $\bar{u}\varphi$ with φ a non-negative test function, since $\bar{u} = \eta'(u)$

We may apply the G^2 method to (75) seeking a piecewise polynomial approximation $\bar{U}$ of $\bar{u}$ in some finite element space $\bar{V}$. In this case we may choose as a discrete test function $\bar{v} = \bar{U} \in \bar{V}$, from which the global form of the entropy inequality follows. Choosing further $\bar{v} = \pi_h(\bar{U}\varphi)$, and using the interpolation estimate (referred to as “super-approximation" because no derivative of U appears)

$$\|\bar{U}\varphi - \pi_h(\bar{U}\varphi)\| \leq C_\varphi \|h\bar{U}\|, \tag{76}$$

we obtain entropy consistency of the G^2-method, this time without using the artificial viscosity term. We conclude that in the G^2 method in entropy variables, the entropy condition is more directly built in because it results from multiplication with the entropy variable $\bar{U}$ itself.

4.3 Dual solution and stability factors in 1d

We apply the simplest Sd(1,0) method in explicit form erefexplversion1 to the standard Riemann problem suggested by Sod, consisting of a rarefaction, contact discontinuity, and a shock, We obtain the following approximate solution on a uniform mesh with $h = 10^{-3}$ and time step 10^{-4} (at time T=0.2055)

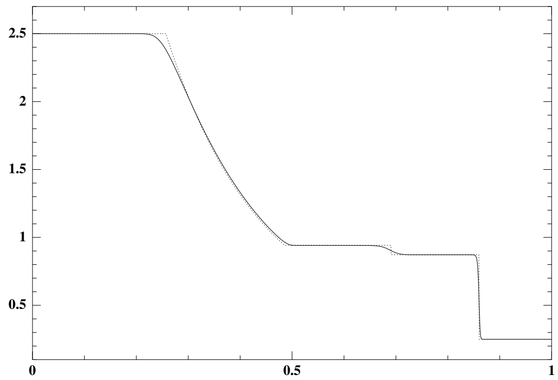

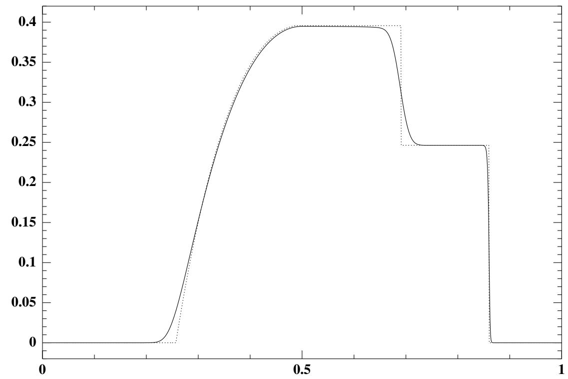

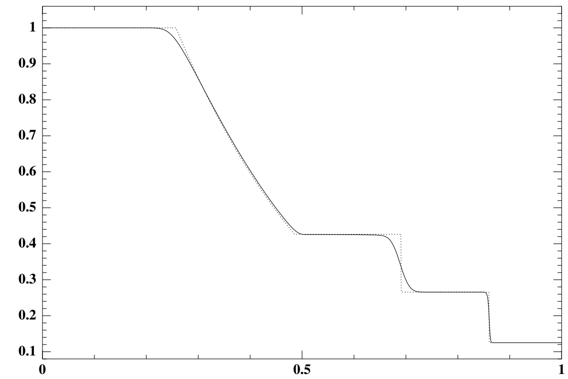

We notice the sharp resolution of the shock, and the smearing of the contact discontinuity (and the rarefaction) caused by the first order artificial viscosity in this variant. The smearing is much smaller in the chG(1,0) and orG(1,0) variants.

The dual solutions take the following form at $t = T$, $t = 0.9T$, $t = 0.5T$, $t = 0$:

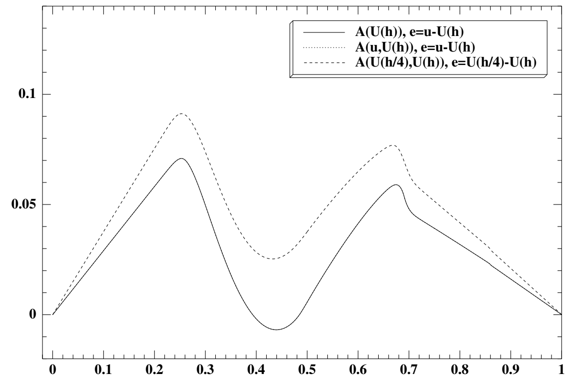
A(U(h)), e=u-U(h)
A(u,U(h)), e=u-U(h)
A(U(h/4),U(h)), e=U(h/4)-U(h)
0.1
0.05
0
0 0.1 0.2 0.3 0.4 0.5 0.6 0.7 0.8 0.9 1

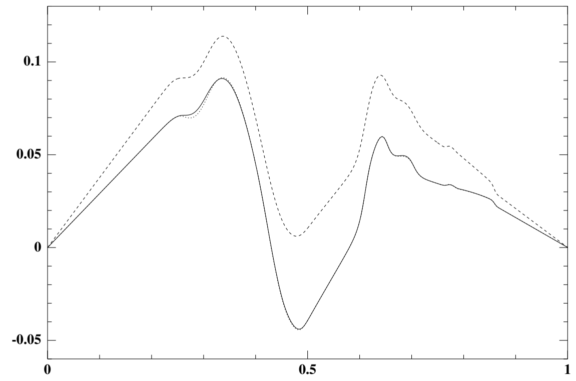
0.1
0.05
0
-0.05
0 0.5 1

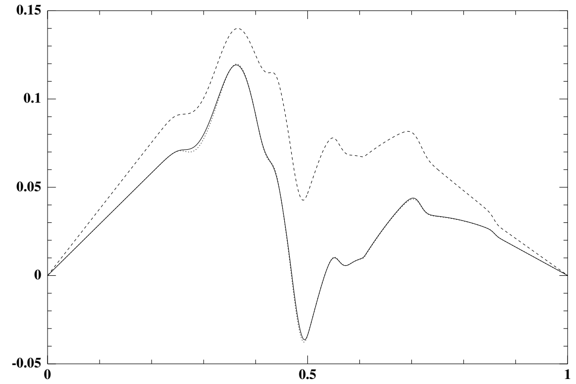
0.15
0.1
0.05
0
-0.05
0 0.5 1

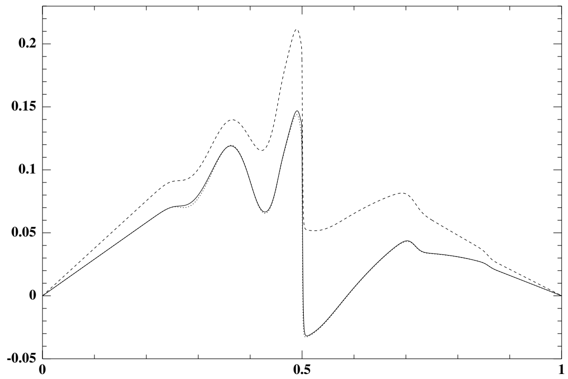

We next plot the corresponding second derivatives :

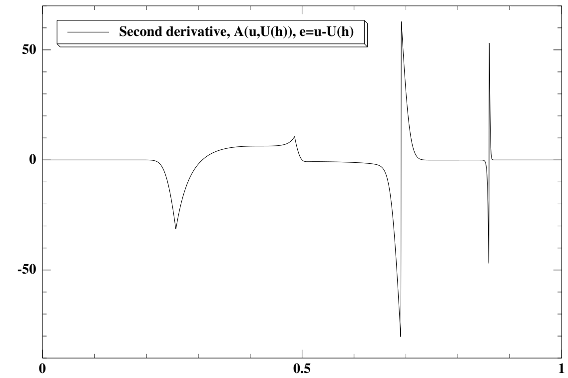

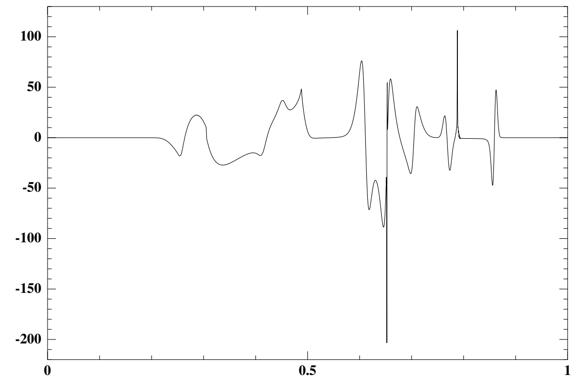

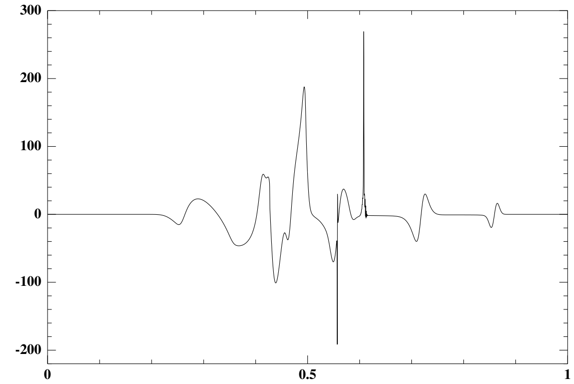

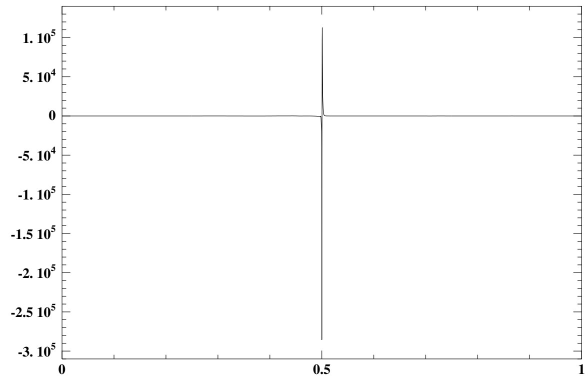

We compare the curves the different approaches at time t=0.9T and t=0.5T:

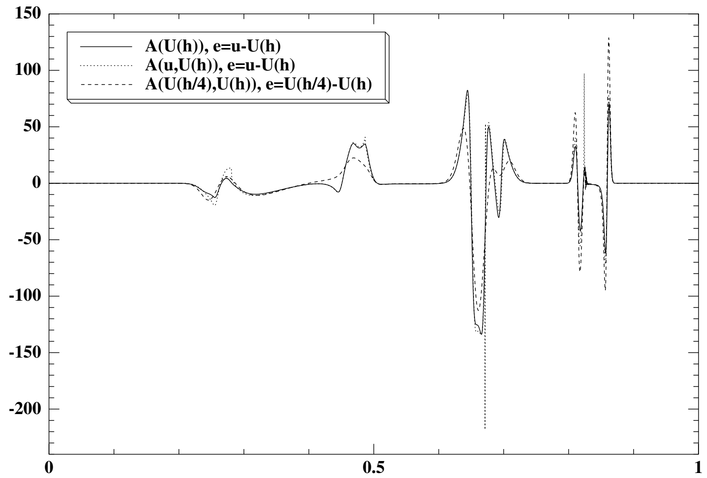

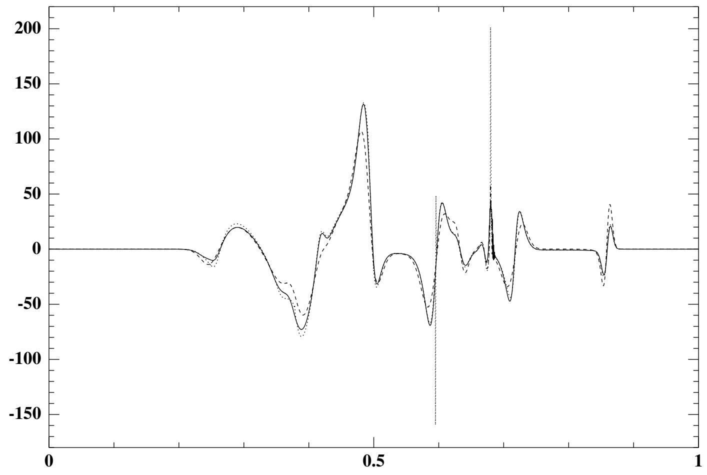

We finally plot the stability factors defined by (60) for different ϵ:

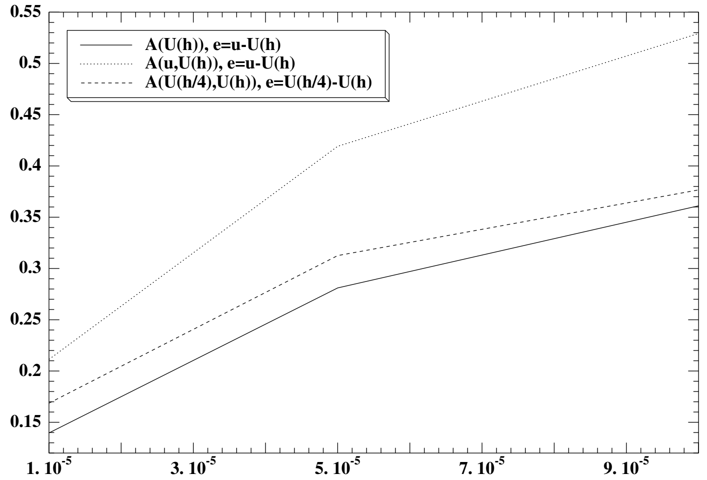

5 The Navier-Stokes equations for viscid compressible flow

The Navier-Stokes equations for a compressible viscous (Newtonian) fluid is the following generalization of the Euler equations (66):

$$\begin{aligned} \dot{u} + \textstyle\sum_{i=1}^3 f_i(u)_{,i} + \sum_{i=1}^3 f_i^v(u)_{,i} = 0 \quad & x \in \mathbb{R}^3,\, t > 0, \\ u(x,0) = u_0(x) \quad & x \in \mathbb{R}^3, \end{aligned} \tag{77}$$

where the f_i^v are diffusive fluxes is a given by

$$f_i^v = \begin{bmatrix} 0 \\ \tau_{1i} \\ \tau_{2i} \\ \tau_{3i} \\ \sum_i \tau_{ij} w_j \end{bmatrix},$$

where the τ_{ij} are viscous stresses given by

$$\tau_{ij} = 2\mu\epsilon_{ij}(w) + \lambda\nabla \cdot w\delta_{ij} \tag{78}$$

with μ and λ parameters.

6 Reactive compressible flow

We consider a fluid mixture of N species, which may undergo M chemical reactions. The Euler equations (66) generalize to

$$\begin{aligned} \dot{u} + \textstyle\sum_{i=1}^{3} f_i(u)_{,i} &= S(u) \quad x \in \mathbb{R}^3, t > 0, \\ u(x,0) &= u_0(x) \quad x \in \mathbb{R}^3, \end{aligned} \tag{79}$$

where

$$u = \rho \begin{bmatrix} y_1 \\ \cdot \\ \cdot \\ y_N \\ w_1 \\ w_2 \\ w_3 \\ e \end{bmatrix}, \; f_i = w_i u + p \begin{bmatrix} 0 \\ \cdot \\ \cdot \\ 0 \\ \delta_{1i} \\ \delta_{2i} \\ \delta_{3i} \\ w_i \end{bmatrix} - \begin{bmatrix} q_i^{D,1} \\ \cdot \\ \cdot \\ q_i^{D,N} \\ 0 \\ \cdot \\ \cdot \\ 0 \\ q_i \end{bmatrix},$$

where ρ is the mixture density, y_i is the mass-fraction for species i, $q = (q_j)$ is the mixture heat flux and $q^{D,i}$ is the diffusive flux for species i, given by

$$q = -\kappa\nabla(\rho c_v T), \qquad q^{D,i} = -D_i \nabla \rho_i$$

where κ and the D_i are diffusion coefficients, and c_v a heat capacity, and finally $S(u) = [s_1 \cdot \cdot s_N \, 0 \cdot \cdot 0]^*$ is a reaction term, typically given by

$$s_i = W_i \sum_{k=1}^{M} (\nu''_{i,k} - \nu'_{i,k}) B_k T^{\alpha_k} e^{-\frac{E_{\alpha,k}}{RT}} \prod_{j=1}^{N} (\frac{X_j p}{RT})^{\nu'_{j,k}}$$

where W_i is the molecular weight of species i, $\nu'_{i,k}$, and $\nu''_{i,k}$ are stoichiometric coefficients, $E_{\alpha,k}$ represents an activation energy, and $B_k T^{\alpha_k}$ is the frequency factor for reaction step k,

$$X_i = \frac{\frac{y_i}{W_i}}{\sum_j \frac{y_j}{W_j}}$$

is the mole fraction of species i, and finally

$$p = \rho RT \sum_i \frac{y_i}{W_i}.$$

The Navier-Stokes equations (77) generalize similary.

The $\mathbf{G^2}$-method and a posteriori estimation The G^2-method for (66) directly generalizes to (77) and (79) including viscous variants, see [37], [2], [3]. As an example we present the Sd-method. Let $\{S_n\}$ be a sequence of space-time slabs $S_n = \mathbb{R}^3 \times I_n$, where $I_n = (t_{n-1}, t_n)$, with associated space-time piecewise polynomials $V_n \subset [\mathcal{C}(S_n)]^{N+4}$, and let $V = \prod_{n\geq 1} V_n$. The Sd-method for (79) reads: find $U \in V$ such that for $n = 1, 2, ...,$

$$\begin{aligned}&(\dot{U} + \textstyle\sum_i A_i(U)U_{,i}, v + \delta(\dot{v} + \sum_i A_i^*(U)v_{,i}))_n \\ &+(\hat{\epsilon}\nabla U, \nabla v)_n + ([U_{n-1}], v_{n-1}^+) \\ &= (S(U), v + \delta(\dot{v} + \textstyle\sum_i A_i^*(U)v_{,i}))_n \quad \forall v \in V_n,\end{aligned}$$

where

$$\delta^* = \delta(U)^* = \frac{1}{2}(k_n^{-2}I + h_n^{-2}\sum_{i=1}^{3} A_i(U)^2)^{-\frac{1}{2}} \quad \text{on } S_n,$$

$$\hat{\epsilon} = \max(\gamma_1 h^2 |R(U)|, \gamma_2 h^{3/2}),$$

$$R(U) = |\dot{U} + \sum_i A_i(U)U_{x_i}| + |[U^n]|/k_n \quad \text{on} \quad S_n.$$

For explicit formulas for the computation of δ, we refer to [37]. The a posteriori error estimatation technique generalizes directly. Again, the main issue is the size of the stability factors S_c. As indicated, in three dimensions these factors may be expected to increase with decreasing viscosity as the complexity of the solutions increase and eventually turbulence develops. Computational results in two dimensions are presented in [37] and in [3]. For computational results on stability factors for incompressible flow, we refer to [34].

7 Conclusion

We have given evidence that a general framework for the numerical solution of conservation laws including the basic concepts of reliability and efficiency, may be develped on the basis of generalized Galerkin methods. A fundamental role is played by a posteriori error estimates involving certain computable stability factors or weights. The computational work required to reach a certain error tolerance increases with increasing stability factors. We have given theoretical and numerical evidence that for problems in one dimension, stability factors typically are of moderate size even for small viscosities, and accordingly solutions in general are computable with work compared to that of direct interpolation. In three dimensions stability factors are expected to increase with decreasing viscosity. In [30], we show that stability factors are inversely proportional to the viscosity in the basic case of parallel flow in three dimensions. As the viscosity decreases, ultimately solutions in three dimensions in general become turbulent and corresponding stability factors are very large. To obtain models with computable solutions, turbulence modeling is required, where on the one hand the effective viscosity is larger and stability factoirs smaller, and on the other hand the modeling error (in suitable weak norms) is controled quantitatively. The design of turbulence models is a major open problem, where computational techniques today open new possibilities. In particular, the techniques presented in this note of a posteriori error estimation, opens the possibility of separating and controling computational and modeling errors.

References

1. S. Bertoluzza, F. Brezzi, C. Johnson and A. Russo, *Dynamic computational subgrid modeling*, Laboratorio Analisi Numerica, Univ of Pavia/Chalmers Finite Element Center. To appear 1997
2. E. Burman, *Adaptive finite element methods for two-phase flow*, Licentiate Thesis, Department of Mathematics, Chalmers University of Technology, Göteborg, 1996.
3. E. Burman, *Adaptive finite element methods for two-phase flow*, Ph d Thesis, Department of Mathematics, Chalmers University of Technology, Göteborg, to appear 1996.
4. K. Eriksson, D. Estep, P. Hansbo and C. Johnson, *Computational Differential Equations*, Cambridge University Press/Studentlitteratur, 1996.
5. ———, *Introduction to Computational Mathematical Modeling*, to appear 1998.
6. ———, *Introduction to Engineering Mathematics*, to appear 1999.
7. ———, *Advanced Computational Differential Equations*, to appear 1998.
8. ———, *Adaptive methods for differential equations*, Acta Numerica, 1995.
9. K. Eriksson and C. Johnson, *Adaptive finite element methods for parabolic problems I: A linear model problem*, SIAM J. Numer. Anal., 28 (1991), pp. 43–77.
10. ———, *Adaptive finite element methods for parabolic problems II: Optimal error estimates in $L_\infty L_2$ and $L_\infty L_\infty$*, SIAM J. Numer. Anal., 32 (1995), pp. 706–740.
11. ———, *Adaptive finite element methods for parabolic problems III: Time steps variable in space*. To appear.
12. ———, *Adaptive finite element methods for parabolic problems IV: Non-linear problems*, SIAM J. Numer. Anal., 32 (1995), pp. 1729–1749.
13. ———, *Adaptive finite element methods for parabolic problems V: Long-time integration*, SIAM J. Numer. Anal., 32 (1995), pp. 1750–1763.
14. ———, *Adaptive finite element methods for parabolic problems VI: Analytic semigroups* , Preprint #1996-32, Department of Mathematics, Chalmers University of Technology, to appear in Siam J. Numer. Anal.
15. ———, *Adaptive streamline diffusion finite element methods for stationary convection-diffusion problems*, Math. Comp., 60 (1993), pp. 167–188.

16. D. Estep, *A posteriori error bounds and global error control for approximations of ordinary differential equations*, Siam J.Numer. Anal. 32 (1995), 1-48.
17. C. Johnson and D. Estep, *On the computability of the Lorenz system*, to appear in M3AS.
18. D. Estep, M. Larson and R. Williams, *Estimating the error of numerical solutions of nonlinear reaction-diffusion equations*, 1997.
19. P. Hansbo, *The characteristic streamline diffusion method for convection-diffusion problems*, Comput. Methods Appl. Mech. Engrg., 96 (1992), pp. 239–253.
20. ———, *The characteristic streamline diffusion method for the time-dependent incompressible Navier-Stokes equations*, Comput. Methods Appl. Mech. Engrg., 99 (1992), pp. 171–186.
21. ———, *Explicit streamline diffusion finite element methods for the compressible Euler equations in conservation variables*, J. Comput. Phys., (1993). In press.
22. ———, *Space-time oriented streamline diffusion methods for nonlinear conservation laws in one dimension*, Commun. Numer. Methods Engrg., (1993). In press.
23. P. Hansbo and C. Johnson, *Adaptive streamline diffusion finite element methods for compressible flow using conservation variables*, Comput. Methods Appl. Mech. Engrg., 87 (1991), pp. 267–280.
24. P. Hansbo and A. Szepessy, *A velocity-pressure streamline diffusion finite element method for the incompressible Navier-Stokes equations*, Comput. Methods Appl. Mech. Engrg., 84 (1990), pp. 175–192.
25. ———, *A new approach to algorithms for convection problems based on exact transport + projection*, Comput. Methods Appl. Mech. Engrg., 100 (1992), pp. 45–62.
26. ———, *Discontinuous Galerkin finite element methods for second order hyperbolic problems*, Comput. Methods Appl. Mech. Engrg., 107 (1993), pp 117-129.
27. C. Johnson and P. Hansbo, *Adaptive finite element methods for small strain elasto-plasticity*, in Finite Inelastic Deformations - Theory and Applications, D. Besdo and E. Stein, eds., Springer, Berlin, 1992, pp. 273–288.
28. ———, *Adaptive finite element methods in computational mechanics*, Comput. Methods Appl. Mech. Engrg., 101 (1992), pp. 143–181.
29. C. Johnson and A. Logg, *Mechlab*, to appear.
30. C. Johnson, R. Rannacher, and M. Boman, *Numerics and hydrodynamic stability: Towards error control in CFD*, SIAM J. Numer. Anal. 32 (1995), pp. 1058-1079.
31. C. Johnson, R. Rannacher, and R. Becker, *Adaptive multigrid methods.* 1995.
32. C. Johnson and A. Szepessy, *Adaptive finite element methods for conservation laws based on a posteriori error estimates*, Comm Appl Pure Math. XLVIII (1995], 199-234.
33. ———, *Convergence of the Discontinuous Galerkin method for scalar conservation laws*, M3AS, 1996.
34. M. Larson, *Analysis of adaptive finite element methods*, Ph D Thesis, Department of Mathematics, Chalmers University of Technology, Göteborg, 1997.
35. M. Levenstam, *Adaptive finite element simulation of welding*, Department of Mathematics, Chalmers University of Technology, Göteborg.

36. P. Möller and P. Hansbo, *On advancing front mesh generation in three dimensions*, Preprint #1993-33, Department of Mathematics, Chalmers University of Technology, 1993.
37. R. Sandboge, *Adaptive finite element methods for reactive flow*, Ph D Thesis, Department of Mathematics, Chalmers University of Technology, Göteborg, 1997.